

A Factor-Graph Approach to Algebraic Topology, With Applications to Kramers–Wannier Duality

Ali Al-Bashabsheh and Pascal O. Vontobel, *Senior Member, IEEE*

Abstract—Algebraic topology studies topological spaces with the help of tools from abstract algebra. The main focus of this paper is to show that many concepts from algebraic topology can be conveniently expressed in terms of (normal) factor graphs. As an application, we give an alternative proof of a classical duality result of Kramers and Wannier, which expresses the partition function of the two-dimensional Ising model at a low temperature in terms of the partition function of the two-dimensional Ising model at a high temperature. Moreover, we discuss analogous results for the three-dimensional Ising model and the Potts model.

Index Terms—Algebraic topology, boundary operator, chain complex, graphical models, factor graphs, factor-graph duality, Ising model, Kramers–Wannier duality, partition function, Potts model.

I. INTRODUCTION

General topology (also known as point-set topology) studies transformation-invariant properties of topological spaces. For example, a mug-shaped object can be smoothly transformed into a doughnut-shaped object, and so general topology does not study the exact details of a given mug-shaped object, but only the properties that are maintained after the mug-shaped object has been smoothly transformed into a doughnut-shaped object.

A particular approach to topology is based on abstract algebra and results in what is known as algebraic topology (see, e.g., [2]–[4]). The power of algebraic topology comes from the vast amount of results available in abstract algebra, in particular about vector spaces.¹ As we will see in this paper, central objects of algebraic topology are vector spaces associated with topological spaces, along with boundary operators and coboundary operators defined on these vector spaces. Homology is then the study of certain quotient spaces based on images and kernels of the boundary operators. On the other hand, cohomology is the study of certain quotient spaces

based on images and kernels of the coboundary operators. The importance of homology and cohomology comes from the fact that the dimensions of the above-mentioned quotient spaces are invariants of a topological space.

In this paper we show how these objects can be conveniently represented with the help of normal factor graphs [5]–[7]. Besides this representation being of inherent interest, the power of this approach comes from the fact that one can apply various known results from the factor-graph literature to study the resulting factor graphs, in particular, one can apply various duality results (see, e.g., [7], [8]).

Of particular interest in this paper are topological spaces where the above-mentioned quotient spaces are trivial or low dimensional.

- Consider first the case where one of these quotient spaces is trivial, which implies that certain two vector spaces are equal. This equality of two vector spaces is interesting because these two vector spaces have typically rather different looking representations in terms of factor graphs. Now, assume to have a factor graph representing one of the two vector spaces. The above observation allows one to replace this factor graph by a factor graph representing the other vector space. As mentioned in the next paragraph, such a replacement can be beneficially used in the study of certain types of factor graphs.
- Consider now the case where one of the above-mentioned quotient spaces is low dimensional, but not trivial. Similar observations as above can be made, however, one factor graph is now replaced by a small number of factor graphs. As we will see, also this replacement can be beneficially used in the study of certain types of factor graphs.

As an application of our factor-graph approach to algebraic topology, we show how the Kramers–Wannier duality [9] (see also [10], [11]), which expresses the partition function of the two-dimensional Ising model [12] at a low temperature in terms of the partition function of the two-dimensional Ising model at a high temperature, can be re-proven with the tools introduced in this paper. As a quick preview, Fig. 13 summarizes our approach to proving the Kramers–Wannier duality: first, we will apply a “Fourier transform” step (which amounts to using Fourier duality results for factor graphs) and then we will apply a “change of support NFG” step (which amounts to using the observations made in the previous paragraph). In our opinion, the resulting proof is easier than existing proofs and gives additional insights.

The fact that one can express the partition function of a statistical model at a low temperature in terms of the partition function of the same or another statistical model at a high temperature is very valuable because frequently it

Manuscript received June 30, 2016; revised June 22, 2017 and December 27, 2017; accepted April 5, 2018. This paper was presented in part at the 2015 IEEE International Symposium on Information Theory [1].

A. Al-Bashabsheh was with the Institute of Network Coding, The Chinese University of Hong Kong, Shatin, Hong Kong. He is now with the Beijing Advanced Innovation Center for Big Data and Brain Computing, Beihang University, Beijing, 100191 (email: entropyali@gmail.com).

P. O. Vontobel is with the Department of Information Engineering and the Institute of Theoretical Computer Science and Communications, The Chinese University of Hong Kong, Shatin, Hong Kong (email: pascal.vontobel@ieee.org).

This work was supported in part by a grant from the University Grants Committee of the Hong Kong SAR, China (Project No. AoE/E-02/08).

¹More generally, algebraic topology can be formulated in terms of modules, however, for our purposes vector spaces are general enough. (Recall that a module is, roughly speaking, a generalization of a vector space where the scalar multiplication by an element in some field is replaced by scalar multiplication by an element in some ring.)

is easier to simulate systems at higher temperatures than at lower temperatures. Overall, note that the Kramers–Wannier duality fits into a more general theme in physics, where some properties of some model are expressed as some other properties of some other model. A very famous, somewhat recent, example is the anti-de Sitter / conformal field theory correspondence, also known as Maldacena duality or gauge / gravity duality [13].

On the side, let us point out that the factor-graph approach to algebraic topology discussed in this paper has recently been used beneficially to study stabilizer quantum codes [14]. Moreover, a recently submitted paper by Forney [15] discusses additional results on how to express objects from algebraic topology in terms of normal factor graphs, with a particular emphasis on coding theory; that paper was motivated by [1] and an earlier version of the present paper.

This paper is structured as follows. In Section II, we review the basics of normal factor graphs (NFGs), in particular also how to obtain the Fourier transform of an NFG. A central part of the present paper are Sections III–IV, where we review notions from algebraic topology and then show how they can be expressed in terms of NFGs. In Section V, we review statistical models, in particular the Boltzmann distribution. We then combine the results of the previous sections toward improving the Kramers–Wannier duality for the two-dimensional Ising model in Section VI. Finally, we consider extensions of Kramer–Wannier type duality results to the three-dimensional Ising model and to the two-dimensional Potts model [16] (see also, e.g., [17]) in Section VII, and conclude the paper in Section VIII.

Throughout this paper, we use calligraphic letters to primarily denote sets. Moreover, \mathbb{F} is some fixed finite field, \mathbb{R} is the field of real numbers, and \mathbb{C} is the field of complex numbers.

II. NORMAL FACTOR GRAPHS

In this section we review, as far as needed for this paper, the basics of normal factor graphs (NFGs) and their Fourier transform. For further background on these topics we refer the interested reader to [5]–[8], [18].

A. NFG definition

We use the following notation. Let \mathcal{E} and \mathcal{X}_e , $e \in \mathcal{E}$, be some finite sets. Based on these sets, we define $\mathcal{X}^{\mathcal{E}} \triangleq \prod_{e \in \mathcal{E}} \mathcal{X}_e$. Frequently, an element of $\mathcal{X}^{\mathcal{E}}$ is denoted by $x_{\mathcal{E}}$ and referred to as a *configuration*. For any configuration $x_{\mathcal{E}}$ and any nonempty $\mathcal{I} \subseteq \mathcal{E}$, we use $x_{\mathcal{I}}$ to denote the components of $x_{\mathcal{E}}$ that are indexed by \mathcal{I} , i.e., $x_{\mathcal{I}} \triangleq (x_i : i \in \mathcal{I})$.

Definition 1 (Normal factor graph). *Consider an undirected (finite) graph with vertex set \mathcal{F} and edge set \mathcal{E} . Based on this graph, we construct an NFG $\mathcal{N} \triangleq (\mathcal{F}, \mathcal{E})$ as follows:*

- with each edge $e \in \mathcal{E}$ we associate a finite alphabet \mathcal{X}_e and a variable x_e taking values from \mathcal{X}_e ;
- and with each vertex $f \in \mathcal{F}$ we associate a (local) function $f(x_{\mathcal{E}(f)})$, where $\mathcal{E}(f)$ is the set of edges incident on f . The degree of a local function f is defined as the degree of f , i.e., the number of edges incident on f . (Note

that we use f as the label of the function node and as the name of the local function.)

We have two types of edges in \mathcal{E} : half-edges, each of which is incident on one vertex, and full-edges, each of which is incident on two vertices. In the following, we will use \mathcal{D} to denote the set of half-edges and $\mathcal{E} \setminus \mathcal{D}$ to denote the set of full-edges. We define

- the global function of the NFG \mathcal{N} to be

$$f_{\mathcal{N}}(x_{\mathcal{E}}) \triangleq \prod_{f \in \mathcal{F}} f(x_{\mathcal{E}(f)}),$$

- and the exterior function of \mathcal{N} to be

$$Z_{\mathcal{N}}(x_{\mathcal{D}}) \triangleq \sum_{x'_{\mathcal{E}}: x'_{\mathcal{D}}=x_{\mathcal{D}}} f_{\mathcal{N}}(x'_{\mathcal{E}}), \quad x_{\mathcal{D}} \in \mathcal{X}_{\mathcal{D}}.$$

If \mathcal{D} is empty, then $Z_{\mathcal{N}}$ is a constant that is called the partition function of the NFG \mathcal{N} . (Clearly, such a constant depends on the local functions. We often allow some of the local functions to depend on some parameter(s), and so $Z_{\mathcal{N}}$ is a function of such parameter(s).)

Throughout the paper, local functions will take on values in \mathbb{R} or \mathbb{C} . With that, the global function and the exterior function will also take on values in \mathbb{R} or \mathbb{C} . ■

Subsequently, we make the following assumption about the variable alphabets. (Many of the upcoming results can be suitably generalized to other scenarios.)

Assumption 2. *We assume $\mathcal{X}_e \triangleq \mathcal{X}$, $e \in \mathcal{E}$, where \mathcal{X} is some finite field \mathbb{F} .* ■

Of common use in the context of NFGs are indicator functions, which are zero/one-valued functions. The following two indicator functions are of particular interest:

- the equality indicator function $\delta_{=}$, which evaluates to one if all its arguments are equal, and to zero otherwise;
- the parity indicator function δ_{+} , which evaluates to one if the sum of its arguments is zero, and to zero otherwise.

The two indicator functions above are marked in the NFG by drawing an “=” or a “+” symbol, respectively, inside the corresponding vertices. Note that an indicator function may be viewed as a constraint on its arguments, and so, for a configuration for which the indicator function evaluates to one, we may say that the indicator function is satisfied.

We say that an NFG \mathcal{N} represents a function f if $Z_{\mathcal{N}}$ equals f up to a (positive) scaling factor, where, whenever possible, we keep track of such a scaling factor in the explicit expression relating f and $Z_{\mathcal{N}}$. Let \mathcal{Y} be some subset of $\mathcal{X}^{\mathcal{D}}$ and let $\delta_{\mathcal{Y}}$ be its indicator function. If \mathcal{N} represents $\delta_{\mathcal{Y}}$, then, for brevity, we say that \mathcal{N} represents the set \mathcal{Y} .

Finally, a small circle marking an edge e incident on a vertex f is adopted to mean that x_e appears negated in the local function f , i.e., such a circle is a shorthand notation of the parity indicator function of degree two.²

²If the characteristic of \mathcal{X} is 2, such markings on the NFG are not necessary since $x = -x$ for all $x \in \mathcal{X}$. However, even for setups where the characteristic of \mathcal{X} is 2 (see, e.g., Section VI about the Ising model), we choose this convention in order to make the discussion general.

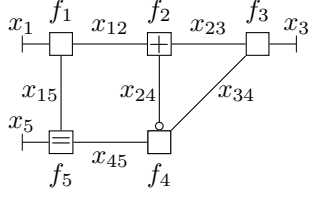


Fig. 1. NFG \mathcal{N} discussed in Example 3.

Example 3. Fig. 1(a) shows an NFG \mathcal{N} , whose global function is given by

$$\begin{aligned} f_{\mathcal{N}}(x_1, \dots, x_{45}) &= f_1(x_1, x_{12}, x_{15}) \cdot f_3(x_3, x_{23}, x_{34}) \\ &\quad \cdot f_4(-x_{24}, x_{34}, x_{45}) \cdot \delta_+(x_{12}, x_{23}, x_{24}) \\ &\quad \cdot \delta_-(x_5, x_{15}, x_{45}). \end{aligned}$$

From the definition of the exterior function it follows that

$$\begin{aligned} Z_{\mathcal{N}}(x_1, x_3, x_5) &= \sum_{x_{12}, x_{23}, x_{34}} f_1(x_1, x_{12}, x_5) \cdot f_3(x_3, x_{23}, x_{34}) \\ &\quad \cdot f_4(x_{12} + x_{23}, x_{34}, x_5). \end{aligned} \quad \triangle$$

Example 4. As another example, Fig. 2(a) shows an NFG \mathcal{N} whose global function is given by

$$\begin{aligned} f_{\mathcal{N}}(x_1, \dots, x''_d) &= f_1(x_1) \cdot f_2(x_2) \cdot f_3(x_3) \cdot f_4(x_4) \cdot f_5(x_5) \cdot \\ &\quad \delta_-(x_a, x'_a) \cdot \delta_-(x_b, x'_b, x''_b) \cdot \delta_-(x_c, x'_c) \cdot \delta_-(x_d, x'_d, x''_d) \cdot \\ &\quad \delta_+(x_1, x'_a, -x_d) \cdot \delta_+(x_2, x_a, -x_b) \cdot \delta_+(x_3, x'_b, -x'_d) \cdot \\ &\quad \delta_+(x_4, x''_b, -x'_c) \cdot \delta_+(x_5, x_c, -x''_d). \end{aligned}$$

One can verify that the NFG's exterior function (which here is also the NFG's partition function) is given by

$$\begin{aligned} Z_{\mathcal{N}} &= \sum_{x_a, x_b, x_c, x_d} f_1(x_d - x_a) \cdot f_2(x_b - x_a) \cdot f_3(x_d - x_b) \cdot \\ &\quad f_4(x_c - x_b) \cdot f_5(x_d - x_c). \end{aligned} \quad \triangle$$

In this work, except for the NFG in Example 3, the NFGs we consider are of a particular form.

Assumption 5. The class of NFGs we are interested in is such that every local function is a parity indicator function or an equality indicator function. In addition to such functions and the edges connecting them, the NFG also contains degree-one (real or complex valued) functions attached to some of the indicator functions. At some places we may replace every degree-one function with a half edge as detailed below. ■

For ease of reference, we define an *interaction function* to be a degree-one local function that is not an indicator function. The motivation for this terminology will become evident as we progress.

Example 6. Figs. 2(a) and (b) show two examples of the NFGs we will see in this work. Both NFGs satisfy Assumption 5. \triangle

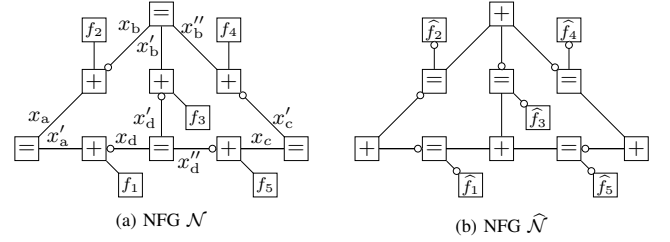


Fig. 2. NFGs discussed in Examples 6, 7, and 14.

Given an NFG $\mathcal{N} = (\mathcal{F}, \mathcal{E})$ as in Assumption 5, we make the following definitions:

- The support NFG of \mathcal{N} , sometimes denoted $\mathcal{N}^\circ = (\mathcal{F}^\circ, \mathcal{E}^\circ)$, is the NFG obtained from \mathcal{N} by cutting out all the interaction functions, i.e., by replacing each interaction function (and its incident edge) with a half-edge. Note that $\mathcal{E}^\circ = \mathcal{E}$, where we assume that full-edges that became half-edges kept their label. The half-edges of \mathcal{N}° will be denoted by \mathcal{D}° .
- The set of (global) *valid* configurations, denoted by $\mathcal{B}_{\mathcal{N}}$, is the set of configurations $x_{\mathcal{E}}$ that satisfy all the indicator functions in \mathcal{N} . (Or, equivalently, all the indicator functions in \mathcal{N}° .)
- The set of projected valid configurations, denoted by $\mathcal{C}_{\mathcal{N}}$, is the projection of the elements of $\mathcal{B}_{\mathcal{N}}$ onto the half-edges of the support NFG of \mathcal{N} , i.e.,

$$\mathcal{C}_{\mathcal{N}} \triangleq \{x_{\mathcal{D}^\circ} : x \in \mathcal{B}_{\mathcal{N}}\}, \quad (1)$$

(If the NFG \mathcal{N} is clear from the context, then $\mathcal{B}_{\mathcal{N}}$ and $\mathcal{C}_{\mathcal{N}}$ might be simplified to \mathcal{B} and \mathcal{C} , respectively.)

Example 7. We continue Example 6. The support NFGs of the NFGs in Figs. 2(a) and (b) are shown in Figs. 2(c) and (d), respectively. \triangle

The importance of the support NFG and the set of projected valid configurations will become clear from subsequent discussions. Note that for any valid configuration $x_{\mathcal{E}}$, the value of the global function, i.e., $f_{\mathcal{N}}(x_{\mathcal{E}})$, depends only on the part of $x_{\mathcal{E}}$ indexed by the edges incident on the interaction functions.

B. Pairwise interaction NFG

As we mentioned in the previous subsection, any NFG in this work will be according to Assumption 5. We also saw in Fig. 2 some NFGs representative of the ones we will see in this work. As discussed in the next subsection, the NFGs in Figs. 2(a) and (c) are intimately related to the ones in Figs. 2(b) and (d), respectively. Namely, given one of the NFGs, the

other NFG is uniquely determined, where we not only have an explicit relation between the local functions of the NFGs, but also an explicit relation between the exterior functions of the NFGs. This motivates naming one of the NFGs and treating it as a primary object, while viewing the other one as a secondary NFG. For reasons that are briefly motivated below, and will become more apparent in subsequent sections, we choose NFGs similar to the NFG in Fig. 2(a) to be the primary NFGs.

The NFG in Fig. 2(a) has a simple interpretation as a physical system. For instance,

- each equality indicator function can be seen (through the equality constraint it imposes on the variables of its incident edges) as a variable representing some physical property of, say, a particle, e.g., spin orientation;
- the degree-one functions can be seen as representing the interaction between neighbouring particles;
- and the parity indicator functions can be seen as restricting attention to systems in which the interaction between neighbouring particles depends only on the difference between the value of the particles' variables.³

In another instance,

- each equality indicator function can be seen as the voltage potential of a site in an electrical network;
- the degree-one functions can be seen as representing the interaction between two sites through an electrical component, e.g., a resistor;
- and the parity indicator functions can be seen as asserting that interactions between adjacent sites depend on the voltage differences between the two sites.

(For more details on electrical networks in this context, we refer the interested reader to [19], where an NFG that resembles Fig. 2(a) was referred to as a “voltage version” factor graph.)

Such a physical system of pairwise interactions can be depicted as a (function) weighted graph $\mathcal{G} = (\mathcal{V}, \mathcal{A})$ with vertex set \mathcal{V} and directed edge set \mathcal{A} as shown in Fig. 3 for the example NFG \mathcal{N} in Fig. 2(a). For such a graph, we associate with every vertex $v \in \mathcal{V}$ the variable x_v , and with every directed edge $a_i = (u, v) \in \mathcal{A}$ the weight $f_i(x_v - x_u)$, where f_i is the corresponding interaction function. (The directedness of the edge reflects the fact that an interaction function might not necessarily be symmetric, i.e., $f_i(-x) \neq f_i(x)$, in general.)

With this, the weighted graph \mathcal{G} can be constructed from the NFG \mathcal{N} as follows.

- Replace each equality indicator function in \mathcal{N} with a vertex v in \mathcal{G} and associate with such a vertex a variable x_v .
- Replace each parity indicator function, its incident edges, and interaction function in \mathcal{N} with an edge $a \triangleq (u, v)$ in \mathcal{G} , where u and v are the vertices in \mathcal{G} that correspond to the (equality) neighbours of the parity indicator function in \mathcal{N} . The edge is directed towards the variable that

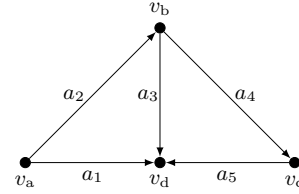


Fig. 3. The corresponding weighted directed graph of the NFG in Fig. 2(a).

appears negated in the parity indicator function. Finally, with f denoting the interaction function in hand, the edge is assigned the weight $f(x_v - x_u)$.

It is clear that the above procedure is reversible, i.e., given \mathcal{G} , we can recover \mathcal{N} in the obvious way. Moreover, note that we can now express the partition function of \mathcal{N} in terms of $\mathcal{G} = (\mathcal{V}, \mathcal{A})$ as

$$Z_{\mathcal{N}} = \sum_{x_{\mathcal{V}}} \prod_{a_i=(u,v) \in \mathcal{A}} f_i(x_v - x_u),$$

which is the expression given in Example 4 since $\mathcal{V} = \{v_a, \dots, v_d\}$ and $\mathcal{A} = \{a_1, \dots, a_5\}$.

The above discussion motivates the following definition.

Definition 8. An NFG according to Assumption 5 that resembles Fig. 2(a), i.e., can be associated with a weighted graph according to the above procedure, is referred to as a (pairwise) interaction NFG.⁴ ■

While the main focus of this work is on pairwise interactions, the definition of an interaction NFG can be easily extended to higher-order interactions. In this case, an interaction function is attached to a parity indicator function of a degree that can be larger than three. We will see an example of such NFGs in Section VII-A.

In contrast to the above, the NFG obtained from an interaction NFG as described in the next subsection (e.g., the NFG in Fig. 2(b)) does not seem to have a physical interpretation in general. (Note that in terms of electrical networks, such an NFG can be seen as a “current version” factor graph [19], but it can no longer be regarded as a system of pairwise interactions. In the example of a system of particles' spins, it is not clear what interpretation can be given to such an NFG.) Nevertheless, as will be detailed in place, such an NFG will be very useful as an alternative NFG for approximating the partition function at low temperature (as in sampling-based methods, which perform poorly on the interaction NFG at low temperature), or as an intermediate step in mapping an interaction NFG at low temperature to another interaction NFG at high temperature (as in Kramers–Wannier duality).

Throughout this paper, we make the following assumption.

Assumption 9. All graphs and NFGs in this work are connected graphs, unless specified otherwise.

³One can consider more general interactions where each parity indicator function and its degree-one function are replaced by a bivariate real or complex function. However, this is beyond the scope of this work.

⁴Similar to the interaction functions attached to parity indicator functions, one can also allow degree-one functions to be attached to the equality indicator functions. In the system of particles' spins, such degree-one functions represent the existence of an external field.

C. Fourier transform of an NFG

In this section we give a brief review of the Fourier transform of an NFG [8], [18], [20].

Note that, because of Assumption 2, \mathcal{X} is a finite Abelian group w.r.t. addition. Let $\widehat{x} : \mathcal{X} \rightarrow \mathbb{C} \setminus \{0\}$ be a group homomorphism, i.e., $\widehat{x}(x+y) = \widehat{x}(x) \cdot \widehat{x}(y)$ for all $x, y \in \mathcal{X}$. Such a homomorphism is called a character (on \mathcal{X}). Moreover, the set of all characters, denoted by $\widehat{\mathcal{X}}$, is a group that is isomorphic to \mathcal{X} , where for all $\widehat{x}, \widehat{y} \in \widehat{\mathcal{X}}$, the addition in $\widehat{\mathcal{X}}$ is defined as $(\widehat{x} + \widehat{y})(x) \triangleq \widehat{x}(x) \cdot \widehat{y}(x)$, $x \in \mathcal{X}$. (See, e.g., [21].)

Definition 10. Let $f : \mathcal{X} \rightarrow \mathbb{C}$ be an arbitrary function on \mathcal{X} . The Fourier transform $\widehat{f} : \widehat{\mathcal{X}} \rightarrow \mathbb{C}$ of f is then defined as

$$\widehat{f}(\widehat{x}) \triangleq \sum_{x \in \mathcal{X}} f(x) \cdot \widehat{x}(x). \quad (2)$$

One can show that f is recoverable from \widehat{f} via⁵

$$f(x) = \frac{1}{|\mathcal{X}|} \cdot \sum_{\widehat{x} \in \widehat{\mathcal{X}}} \widehat{f}(\widehat{x}) \cdot \widehat{x}(-x). \quad (3)$$

Let \mathcal{Y} be a subgroup of \mathcal{X} and define

$$\mathcal{Y}^\perp \triangleq \left\{ \widehat{x} \in \widehat{\mathcal{X}} \mid \widehat{x}(x) = 1 \text{ for all } x \in \mathcal{Y} \right\}.$$

One can verify that \mathcal{Y}^\perp is a subgroup of $\widehat{\mathcal{X}}$; it is called the orthogonal subgroup to \mathcal{Y} . Let $\delta_{\mathcal{Y}}$ be the indicator function of \mathcal{Y} , i.e., for all $x \in \mathcal{X}$, the indicator function defined as $\delta_{\mathcal{Y}}(x) = 1$ iff $x \in \mathcal{Y}$. The following fact regarding the Fourier transform of $\delta_{\mathcal{Y}}$ will be useful.

Lemma 11. Let \mathcal{Y} be a subgroup of \mathcal{X} . Then it holds that

$$\widehat{\delta_{\mathcal{Y}}} = |\mathcal{Y}| \cdot \delta_{\mathcal{Y}^\perp}. \quad (4)$$

Proof. See, e.g., [21, Ch. 5]. \square

Example 12. Consider an equality indicator function node and a parity indicator function node of degree d . It is straightforward to verify that there are subgroups $\mathcal{Y}_=$ and \mathcal{Y}_+ of \mathcal{X}^d such that $\delta_= = \delta_{\mathcal{Y}_=}$ and $\delta_+ = \delta_{\mathcal{Y}_+}$, respectively. Moreover, because of $(\mathcal{Y}_=)^\perp = \mathcal{Y}_+$, $|\mathcal{Y}_=| = |\mathcal{X}|$, $|\mathcal{Y}_+| = |\mathcal{X}|^{d-1}$, and Lemma 11, we have

$$\begin{aligned} \widehat{\delta}_= &= |\mathcal{X}| \cdot \delta_+, \\ \widehat{\delta}_+ &= |\mathcal{X}|^{d-1} \cdot \delta_=, \end{aligned} \quad (5)$$

\triangle

Remark 13 (Fourier-transformed NFG). Given an NFG \mathcal{N} , the Fourier-transformed NFG $\widehat{\mathcal{N}}$ can be obtained as follows:

- 1) Insert a degree-two parity indicator function on each internal edge.
- 2) Replace each local function with its Fourier transform.⁶

⁵This follows from the well-known fact that for two characters $\widehat{x}_1, \widehat{x}_2 \in \widehat{\mathcal{X}}$ the expression $\sum_x \widehat{x}_1(x) \cdot \widehat{x}_2(-x)$ evaluates to $|\mathcal{X}|$ if $\widehat{x}_1 = \widehat{x}_2$ and to 0 otherwise.

⁶Frequently, we will replace a local (indicator) function not by its Fourier transform but by a scaled version of its Fourier transform, and separately keep track of the product of all the omitted scaling factors. For example, $\delta_=$ is replaced by δ_+ (not by $|\mathcal{X}| \cdot \delta_+$) and the omitted scaling factor $|\mathcal{X}|$ is dealt with separately. Similarly, δ_+ is replaced by $\delta_=$ (not by $|\mathcal{X}|^{d-1} \cdot \delta_=$) and the omitted scaling factor $|\mathcal{X}|^{d-1}$ is dealt with separately.

- 3) As far as needed in order to be explicit, associate suitable variables with the edges in $\widehat{\mathcal{N}}$.

The exterior functions of \mathcal{N} and $\widehat{\mathcal{N}}$ are related as follows [8]

$$\widehat{Z}_{\mathcal{N}}(\widehat{x}_{\mathcal{D}}) = \frac{1}{\prod_{e \in \mathcal{E} \setminus \mathcal{D}} |\mathcal{X}_e|} \cdot Z_{\widehat{\mathcal{N}}}(\widehat{x}_{\mathcal{D}}). \quad (6)$$

In particular, when there are no half edges, $Z_{\mathcal{N}}$ and $Z_{\widehat{\mathcal{N}}}$ are equal, up to a scaling factor, i.e., $Z_{\mathcal{N}} = \frac{1}{\prod_{e \in \mathcal{E}} |\mathcal{X}_e|} \cdot Z_{\widehat{\mathcal{N}}}$. (The expression in (6) assumes that local functions are replaced by their Fourier transform in Step 2. If the procedure outlined in Footnote 6 is applied, then the scaling factor in (6) needs to be suitably adjusted.) \triangle

Example 14. Fig. 2(b) shows the Fourier transform of the NFG in Fig. 2(a). Note that we have taken advantage of the procedure outlined in Footnote 6. \triangle

The next theorem is a specialization of (6) customized to the NFGs in this work.

Theorem 15. Let \mathcal{N} be an interaction NFG as in Definition 8 and $\widehat{\mathcal{N}}$ be its Fourier-transformed NFG, then

$$\mathcal{C}_{\mathcal{N}} = (\mathcal{C}_{\widehat{\mathcal{N}}})^\perp. \quad (7)$$

Moreover, with the scaling factors of the indicator functions omitted in $\widehat{\mathcal{N}}$ (see Footnote 6), we have

$$Z_{\mathcal{N}} = \frac{1}{|\mathcal{X}|^{|\mathcal{A}|-|\mathcal{V}|}} \cdot Z_{\widehat{\mathcal{N}}}, \quad (8)$$

or more explicitly,

$$|\mathcal{X}| \cdot \sum_{x_{\mathcal{A}} \in \mathcal{C}_{\mathcal{N}}} \prod_{e \in \mathcal{A}} f_e(x_e) = \frac{1}{|\mathcal{X}|^{|\mathcal{A}|-|\mathcal{V}|}} \cdot \sum_{x_{\mathcal{A}} \in (\mathcal{C}_{\widehat{\mathcal{N}}})^\perp} \prod_{e \in \mathcal{A}} \widehat{f}_e(x_e), \quad (9)$$

where $(\mathcal{V}, \mathcal{A})$ is the weighted graph obtained from \mathcal{N} using the procedure above Definition 8. \blacksquare

Proof. We prove (7) by observing that

$$\begin{aligned} \delta_{\mathcal{C}_{\widehat{\mathcal{N}}}} &= c \cdot Z_{(\widehat{\mathcal{N}})^\circ} = c \cdot Z_{(\widehat{\mathcal{N}}^\circ)} \\ &\stackrel{(6)}{=} c' \cdot \widehat{Z}_{\mathcal{N}^\circ} = c'' \cdot \widehat{\delta}_{\mathcal{C}_{\mathcal{N}}} \stackrel{(4)}{=} c''' \cdot \delta_{(\mathcal{C}_{\mathcal{N}})^\perp}, \end{aligned}$$

where c, \dots, c''' are scaling factors, and where the unlabelled equalities follow directly from the definition of the support NFG. Equation (8) follows from (6) and (5) by noting that, in \mathcal{N} , there are $3 \times |\mathcal{A}|$ full edges and no half edges, and that there are $|\mathcal{V}|$ equality-indicator functions and $|\mathcal{A}|$ parity-indicator functions (each of degree three). Finally, $Z_{\mathcal{N}}$ is equal to the l.h.s. of (9), which is clear by noting that only a valid configuration contributes to $Z_{\mathcal{N}}$ and such a contribution depends only on the corresponding projection in $\mathcal{C}_{\mathcal{N}}$. The scaling factor $|\mathcal{X}|$ appears because there are $|\mathcal{X}|$ valid configurations that have the same projection x for all $x \in \mathcal{C}_{\mathcal{N}}$. (Here we used Assumption 9.) The r.h.s. of (9) follows from (7) and (8) by noting that $Z_{\widehat{\mathcal{N}}} = \sum_{x_{\mathcal{A}} \in \mathcal{C}_{\widehat{\mathcal{N}}}} \prod_{e \in \mathcal{A}} \widehat{f}_e(x_e)$. (Observe that, in comparison to the argument leading to the l.h.s., the scaling factor here is one since a configuration on the half edges of the support NFG of $\widehat{\mathcal{N}}$ uniquely determines a global configuration on all the edges of such an NFG.) \square

III. 1-COMPLEXES

In this section we introduce 1-complexes. More precisely, Section III-A defines chains, boundary operators, and homology spaces, whereas Section III-C defines the duals of these objects, i.e., cochains, coboundary operators, and cohomology spaces, respectively. For further background on these topics, we refer the interested reader to [2]–[4].

Sections III-A and III-C are complemented by Sections III-B and III-D, where we introduce some NFGs that we associate with boundary and coboundary operators, respectively.

Note that 2-complexes will be introduced in Sections IV. (Higher-order complexes are briefly discussed in Appendix A.)

A. Chains, boundary operators, and homology spaces

Definition 16. Consider a graph $\mathcal{G} \triangleq (\mathcal{V}, \mathcal{A})$ with vertex set \mathcal{V} and edge set \mathcal{A} . We define the following objects:

- $C_0 \triangleq \mathbb{F}^{\mathcal{V}}$, whose elements are called 0-chains;
- $C_1 \triangleq \mathbb{F}^{\mathcal{A}}$, whose elements are called 1-chains.

Note that C_0 is the set of functions from \mathcal{V} to \mathbb{F} , and C_1 is the set of functions from \mathcal{A} to \mathbb{F} . We can also think of C_0 to be a $|\mathcal{V}|$ -dimensional vector space over \mathbb{F} and of C_1 to be an $|\mathcal{A}|$ -dimensional vector space over \mathbb{F} .

With a 0-chain $x \in \mathbb{F}^{\mathcal{V}}$ we associate the formal sum

$$x \triangleq \sum_{v \in \mathcal{V}} x(v) \cdot v. \quad (10)$$

Similarly, with a 1-chain $y \in \mathbb{F}^{\mathcal{A}}$ we associate the formal sum

$$y \triangleq \sum_{a \in \mathcal{A}} y(a) \cdot a. \quad (11)$$

With the above associations, we can view \mathcal{V} and \mathcal{A} as (standard) bases of $\mathbb{F}^{\mathcal{V}}$ and $\mathbb{F}^{\mathcal{A}}$, respectively. (Here, for every $v \in \mathcal{V}$, the vertex v is associated with the 0-chain $1 \cdot v \in \mathbb{F}^{\mathcal{V}}$, with a similar statement for the edges $a \in \mathcal{A}$.) ■

In the following, for every $a \in \mathcal{A}$ we fix a direction.⁷ We will write $a = (v, v')$ if the direction of the edge a has been chosen such that the edge starts at vertex v and ends at vertex v' . For such an edge a , the boundary vertices are v and v' . We formalize this as follows.

Definition 17. The boundary operator $\partial_1 : C_1 \rightarrow C_0$, which maps 1-chains to 0-chains, is defined to be the (unique) linear map which satisfies

$$\text{for every } a = (v, v') \in \mathcal{A}: \quad \partial_1(a) \triangleq v' - v. \quad \blacksquare$$

We see that $\partial_1(a)$ not only gives the boundary vertices of a directed edge a , but also tells us which boundary vertex is the starting vertex and which boundary vertex is the ending vertex,

⁷Although some of the resulting calculations will be different for different choices of directions, the quantities that are ultimately of interest, like the dimension of certain quotient spaces, will be independent of this choice of directions.

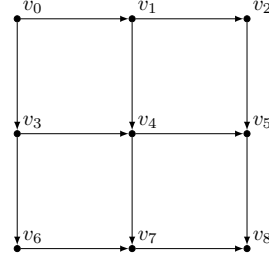


Fig. 4. A graph $\mathcal{G} = (\mathcal{V}, \mathcal{A})$.

namely, the vertices with coefficients -1 and $+1$, respectively. Note that if $a = (v, v')$, then

$$\partial_1(-a) = -\partial_1(a) = -(v' - v) = v - v',$$

i.e., $-a$ represents the directed edge from v' to v .

Example 18. Consider the directed graph in Fig. 4 with $|\mathcal{V}| = 9$ vertices and $|\mathcal{A}| = 12$ edges. In the following, we use a_{ij} to denote the directed edge (v_i, v_j) .

- Boundary of $a_{01} + a_{14} + a_{47}$:

$$\begin{aligned} \partial_1(a_{01} + a_{14} + a_{47}) &= \partial_1(a_{01}) + \partial_1(a_{14}) + \partial_1(a_{47}) \\ &= (v_1 - v_0) + (v_4 - v_1) + (v_7 - v_4) \\ &= v_7 - v_0. \end{aligned}$$

This calculation makes sense because $a_{01} + a_{14} + a_{47}$ represents the concatenation of the directed edges a_{01} , a_{14} , and a_{47} , which is the directed path from starting vertex v_0 to ending vertex v_7 .

- Boundary of $a_{01} + a_{14} + (-a_{34}) + (-a_{03})$:

$$\begin{aligned} \partial_1(a_{01} + a_{14} + (-a_{34}) + (-a_{03})) &= \partial_1(a_{01} + a_{14} - a_{34} - a_{03}) \\ &= \partial_1(a_{01}) + \partial_1(a_{14}) - \partial_1(a_{34}) - \partial_1(a_{03}) \\ &= (v_1 - v_0) + (v_4 - v_1) - (v_4 - v_3) - (v_3 - v_0) \\ &= 0. \end{aligned}$$

Again, this calculation makes sense because $a_{01} + a_{14} + (-a_{34}) + (-a_{03})$ represents the concatenation of the directed edges a_{01} , a_{14} , $-a_{34}$, and $-a_{03}$, which is a directed closed cycle from v_0 to v_0 , and because directed closed cycles have no boundary.

- Boundary of $2a_{67} + 3a_{78}$:

$$\begin{aligned} \partial_1(2a_{67} + 3a_{78}) &= 2 \cdot \partial_1(a_{67}) + 3 \cdot \partial_1(a_{78}) \\ &= 2 \cdot (v_7 - v_6) + 3 \cdot (v_8 - v_7) \\ &= 3v_8 - v_7 - 2v_6. \end{aligned}$$

△

Recall that the kernel (denoted by “ker”) of a linear map is the set of all elements in the domain that map to zero.

Definition 19. The elements of $\ker \partial_1$, i.e., the elements of C_1 with zero boundaries, will be called 1-cycles. ■

Example 20. The second calculation in Example 18 shows that $a_{01} + a_{14} - a_{34} - a_{03}$ is a 1-cycle. Note that any multiple of $a_{01} + a_{14} - a_{34} - a_{03}$ is also a 1-cycle. △

$$C_2 \xrightarrow{\partial_2} C_1 \xrightarrow{\partial_1} C_0 \xrightarrow{\partial_0} C_{-1} \quad (12)$$

$$\widehat{C}_2 \xleftarrow{d_2} \widehat{C}_1 \xleftarrow{d_1} \widehat{C}_0 \xleftarrow{d_0} \widehat{C}_{-1} \quad (13)$$

Fig. 5. Spaces and mappings associated with a 1-complex.

The following definition turns out to be useful for subsequent considerations.

Definition 21. We define the sets $C_2 \triangleq \{0\}$ and $C_{-1} \triangleq \{0\}$, along with the trivial mappings $\partial_2 : C_2 \rightarrow C_1$ and $\partial_0 : C_0 \rightarrow C_{-1}$. ■

The objects that we have introduced so far are summarized in (12); the collection of these objects is known as a 1-dimensional chain complex, or simply 1-complex.

In the following, we will use “im” to denote the image of a map. Because $\text{im } \partial_2 = \{0\}$ and $\ker \partial_0 = C_0$, we clearly have

$$\text{im } \partial_2 \subseteq \ker \partial_1, \quad (14)$$

$$\text{im } \partial_1 \subseteq \ker \partial_0. \quad (15)$$

The fact that there might be a gap between $\text{im } \partial_2$ and $\ker \partial_1$ is captured by the 1-st homology space. Similarly, the fact that there might be a gap between $\text{im } \partial_1$ and $\ker \partial_0$ is captured by the 0-th homology space.

Definition 22. The 1-st and the 0-th homology spaces are defined to be the quotient spaces

$$H_1 \triangleq \ker \partial_1 / \text{im } \partial_2, \quad (16)$$

$$H_0 \triangleq \ker \partial_0 / \text{im } \partial_1, \quad (17)$$

respectively. ■

We now discuss the dimensions of the spaces we have seen so far. We start with H_0 and let $\mathcal{G} = (\mathcal{V}, \mathcal{A})$ be a connected graph.⁸ For an arbitrary $v_0 \in \mathcal{V}$ and any other $v \in \mathcal{V}$, let $y \in C_1$ be a 1-chain corresponding to an oriented path in \mathcal{G} from v_0 to v . (An oriented path is a directed path that contains elements from $\{a, -a \mid a \in \mathcal{A}\}$, where $-a \triangleq (v, u)$ for all $(u, v) \in \mathcal{A}$. The corresponding 1-chain y is such that for all $a \in \mathcal{A}$, $y(a) = 1$, if a is in the oriented path; $y(a) = -1$, if $-a$ is in the oriented path; and $y(a) = 0$, otherwise.) Then,

$$\partial_1 y = v - v_0 \in \text{im } \partial_1,$$

and so, every element v of the basis \mathcal{V} is equivalent to v_0 , modulo $\text{im } \partial_1$. Hence,

$$\dim H_0 = 1. \quad (18)$$

From this and (17), it is immediate that

$$\dim(\text{im } \partial_1) = \dim(\ker \partial_0) - \dim H_0 = |\mathcal{V}| - 1. \quad (19)$$

(Recall that ∂_0 is the zero map.) On the other hand, by the rank-nullity theorem, we have

$$\dim(\ker \partial_1) = |\mathcal{A}| - \dim(\text{im } \partial_1) = |\mathcal{A}| - |\mathcal{V}| + 1, \quad (20)$$

⁸Here we benefited from [22] in first discussing $\dim H_0$ and then $\dim H_1$, instead of the other way around. Such a choice facilitates the arguments and appears more natural.

and so,

$$\dim H_1 = |\mathcal{A}| - |\mathcal{V}| + 1. \quad (21)$$

(Recall that, for a 1-complex, ∂_2 is the zero map.)

To construct a basis for $\text{im } \partial_1$, let $\mathcal{T} \triangleq (\mathcal{V}, \mathcal{A}_{\mathcal{T}})$ be a spanning tree of \mathcal{G} . The 0-chains in the set $\{\partial_1 a : a \in \mathcal{A}_{\mathcal{T}}\}$ are independent since \mathcal{T} contains no cycles, and so, by (19) they form a basis of $\text{im } \partial_1$.

To construct a basis for $\ker \partial_1$, note that each edge $a \in \mathcal{A} \setminus \mathcal{A}_{\mathcal{T}}$ induces an oriented cycle in \mathcal{G} , and so the corresponding 1-chain is a 1-cycle. These 1-cycles are independent since each one involves a different edge from $\mathcal{A} \setminus \mathcal{A}_{\mathcal{T}}$, and so, by (20) they form a basis of $\ker \partial_1$.

Example 23. Continuing with the example graph $\mathcal{G} = (\mathcal{V}, \mathcal{A})$ in Fig. 4, let $\mathcal{T} \triangleq (\mathcal{V}, \mathcal{A}_{\mathcal{T}})$ be a spanning tree of \mathcal{G} , say,

$$\mathcal{A}_{\mathcal{T}} \triangleq \{a_{01}, a_{12}, a_{34}, a_{45}, a_{67}, a_{78}, a_{14}, a_{47}\}.$$

Then the set

$$\{\partial_1(a) \mid a \in \mathcal{A}_{\mathcal{T}}\} = \{v_1 - v_0, v_2 - v_1, \dots, v_7 - v_4\}$$

forms a basis of $\text{im } \partial_1$.

The edges $\mathcal{A} \setminus \mathcal{A}_{\mathcal{T}} = \{a_{03}, a_{25}, a_{36}, a_{58}\}$ induce the cycles

$$c_0 \triangleq a_{01} + a_{14} - a_{34} - a_{03},$$

$$c_1 \triangleq a_{12} + a_{25} - a_{45} - a_{14},$$

$$c_2 \triangleq a_{34} + a_{47} - a_{67} - a_{36},$$

$$c_3 \triangleq a_{45} + a_{58} - a_{78} - a_{47},$$

which form a basis of $\ker \partial_1$. △

The above arguments can be extended to graphs with more than one component. Namely, for a graph \mathcal{G} with $\text{comp}(\mathcal{G})$ components, one can show (see, e.g., [2, p. 425]) that

$$\dim H_0 = \text{comp}(\mathcal{G}),$$

$$\dim H_1 = |\mathcal{A}| - |\mathcal{V}| + \text{comp}(\mathcal{G}).$$

These two quantities are known as the zeroth and first Betti numbers of the graph \mathcal{G} , respectively. (More generally, $\dim H_i$ is called the i -th Betti number.) Moreover, note that $\dim H_1$ is also known as the cyclomatic number of the graph \mathcal{G} , i.e., the minimum number of edges that must be removed in order to make the graph cycle free.

B. NFG representation of the boundary operator

In this subsection we introduce the following NFGs:

- \mathcal{N}_{∂_1} , an NFG whose exterior function is proportional to the indicator function of $\{(y, \partial_1 y) \mid y \in C_1\}$.
- $\mathcal{N}_{\ker \partial_1}$, an NFG whose exterior function is proportional to the indicator function of $\ker \partial_1$.
- $\mathcal{N}_{\text{im } \partial_1}$, an NFG whose exterior function is proportional to the indicator function of $\text{im } \partial_1$.

We start by defining the set

$$\mathcal{B}_{\partial_1} \triangleq \{(y, x) \mid y \in C_1, x = \partial_1 y\},$$

which contains all possible pairs of a 1-chain and its image under ∂_1 . We can rewrite \mathcal{B}_{∂_1} in terms of the bases in Definition 16 as

$$\mathcal{B}_{\partial_1} = \left\{ \left((y(a))_{a \in \mathcal{A}}, (x(v))_{v \in \mathcal{V}} \right) \mid y \in C_1, x = \partial_1 y \right\}. \quad (22)$$

Using this notation, we make the following definition, whose terminology was motivated by analogous objects in [15].

Definition 24. Given a graph $\mathcal{G} = (\mathcal{V}, \mathcal{A})$, we define the input/output NFG \mathcal{N}_{∂_1} associated with ∂_1 to be the NFG that has the following properties:

- For every $a \in \mathcal{A}$, there is an equality indicator function with two full edges and an input (ingoing) half-edge whose associated variable is $y(a)$.
- For every $v \in \mathcal{V}$, there is a parity indicator function with a full edge (possibly with a sign inverter) for every edge incident on v and an output (outgoing) half-edge whose associated variable is $x(v)$.
- The full edges connect the indicator functions in the obvious way, i.e., the parity indicator function of $v \in \mathcal{V}$ is connected to the equality indicator function of $a \in \mathcal{A}$ iff a is incident on v . ■

Example 25. Consider again the graph $\mathcal{G} = (\mathcal{V}, \mathcal{A})$ in Fig. 4. The input/output NFG \mathcal{N}_{∂_1} associated with ∂_1 is shown in Fig. 6(a). \triangle

Lemma 26. Let $\mathcal{G} = (\mathcal{V}, \mathcal{A})$ be some graph and let \mathcal{N}_{∂_1} be the input/output NFG associated with ∂_1 , then

$$Z_{\mathcal{N}_{\partial_1}}(x_{\mathcal{D}}) \propto \delta_{\mathcal{B}_{\partial_1}}(x_{\mathcal{D}}) \quad \text{for all } x_{\mathcal{D}} \in \mathcal{X}_{\mathcal{D}}. \quad (23)$$

Proof. Consider an arbitrary 1-chain y and an arbitrary 0-chain x . Then, we have $(y, x) \in \mathcal{B}_{\partial_1}$ iff

$$\begin{aligned} x &= \partial_1 y = \sum_{a \in \mathcal{A}} y(a) \cdot \partial_1(a) = \sum_{a \triangleq (u,v) \in \mathcal{A}} y(a) \cdot (v - u) \\ &= \sum_{v \in \mathcal{V}} \left(\sum_{a \in \text{In}(v)} y(a) - \sum_{a \in \text{Out}(v)} y(a) \right) \cdot v, \end{aligned} \quad (24)$$

where the second equality follows from (11) and the linearity of ∂_1 , and the last equality is obtained by rearranging the terms in the summation preceding it. Here we used the notation $\text{In}(v)$ and $\text{Out}(v)$ to denote the sets of edges entering and leaving a vertex v , respectively. By the independence of the vertices (in C_0), we have $x = \partial_1 y$ iff $x(v) = \sum_{a \in \text{In}(v)} y(a) - \sum_{a \in \text{Out}(v)} y(a)$ for all $v \in \mathcal{V}$. This constraint (with the output and input half-edges of \mathcal{N}_{∂_1} associated with $x(v), v \in \mathcal{V}$, and $y(a), a \in \mathcal{A}$, respectively) corresponds to the local parity indicator functions in \mathcal{N}_{∂_1} . The equality indicator functions simply account for the fact that each edge is incident on two vertices. Finally, one can verify that the proportionality constant in (23) is given by $\sum_{x_{\mathcal{E}} \in \mathcal{X}_{\mathcal{E}}: x_{\mathcal{D}}=0_{\mathcal{D}}} f_{\mathcal{N}_{\partial_1}}(x_{\mathcal{E}})$, i.e., the number of valid configurations of \mathcal{N}_{∂_1} that are all-zero on the half-edges. \square

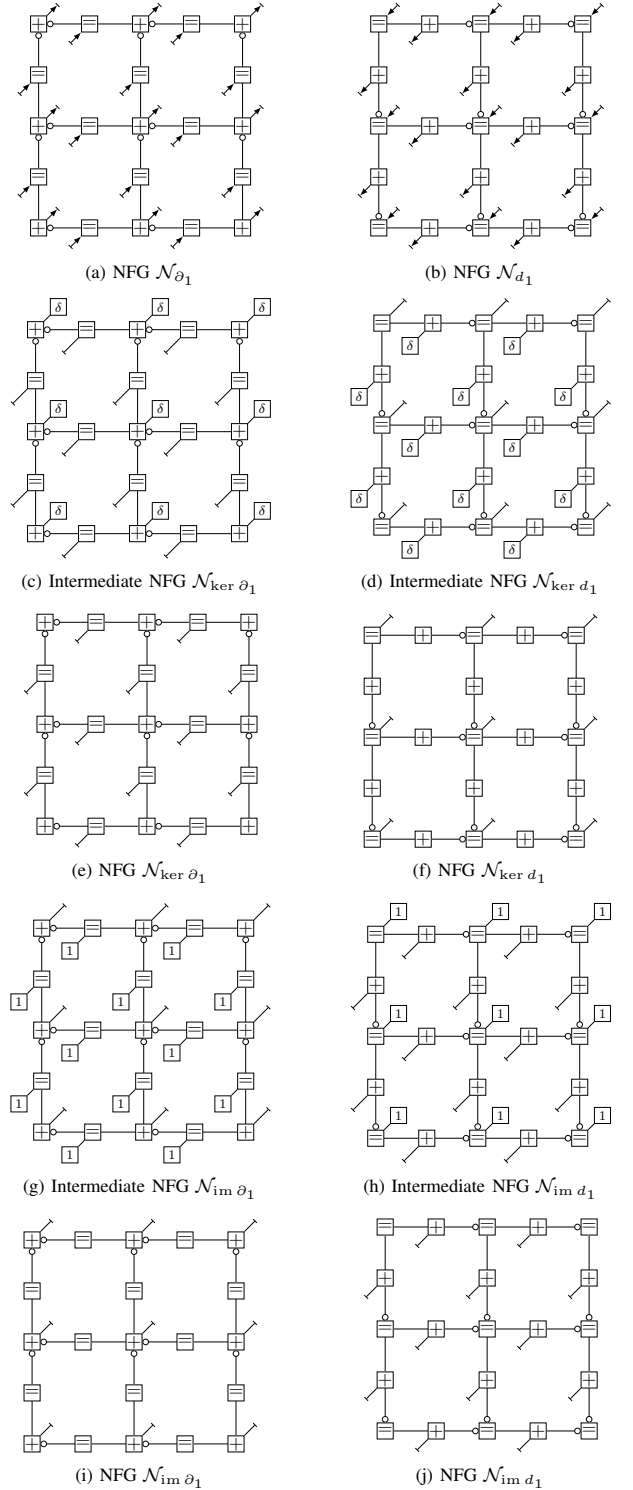


Fig. 6. NFGs associated with the graph $\mathcal{G} = (\mathcal{V}, \mathcal{A})$ in Fig. 4.

We now proceed to define $\mathcal{N}_{\ker \partial_1}$ and $\mathcal{N}_{\text{im } \partial_1}$. Note that coordinate-based representations of $\ker \partial_1$ and $\text{im } \partial_1$ are, respectively,

$$\ker \partial_1 = \left\{ (y(a))_{a \in \mathcal{A}} \mid y \in C_1, \partial_1 y = 0 \right\}, \quad (25)$$

$$\text{im } \partial_1 = \left\{ x \triangleq ((\partial_1 y)(v))_{v \in \mathcal{V}} \mid y \in C_1 \right\}, \quad (26)$$

Definition 27. Given an input/output NFG \mathcal{N}_{∂_1} , we define the NFG $\mathcal{N}_{\ker \partial_1}$ to be the NFG obtained from \mathcal{N}_{∂_1} by deleting all the output half-edges. We also define $\mathcal{N}_{\text{im } \partial_1}$ as the NFG obtained from \mathcal{N}_{∂_1} by deleting all the input-half edges. ■

A lemma similar to Lemma 26 leads to

$$\begin{aligned} Z_{\mathcal{N}_{\ker \partial_1}}(x_{\mathcal{D}}) &\propto \delta_{\ker \partial_1}(x_{\mathcal{D}}), & x_{\mathcal{D}} \in \mathcal{X}_{\mathcal{D}}, \mathcal{D} \triangleq \mathcal{D}_{\mathcal{N}_{\ker \partial_1}}, \\ Z_{\mathcal{N}_{\text{im } \partial_1}}(x_{\mathcal{D}}) &\propto \delta_{\text{im } \partial_1}(x_{\mathcal{D}}), & x_{\mathcal{D}} \in \mathcal{X}_{\mathcal{D}}, \mathcal{D} \triangleq \mathcal{D}_{\mathcal{N}_{\text{im } \partial_1}}. \end{aligned}$$

This follows by noting that the NFG $\mathcal{N}_{\ker \partial_1}$ can be obtained from \mathcal{N}_{∂_1} by attaching function nodes representing Kronecker-delta functions to the output half-edges (see (22) and (25)), thereby, in effect, deleting these half-edges. (More precisely, the NFG $\mathcal{N}_{\ker \partial_1}$ can be obtained from \mathcal{N}_{∂_1} by constructing an intermediate NFG where function nodes representing Kronecker-delta functions are attached to the output half-edges (see (22) and (25)), and then simplifying the intermediate NFG to an NFG having the same exterior function by deleting these Kronecker-delta functions and their incident edges.) Similarly, the NFG $\mathcal{N}_{\text{im } \partial_1}$ can be obtained from \mathcal{N}_{∂_1} by attaching function nodes representing all-one functions to the input half-edges (see (22) and (26)), thereby, in effect, deleting these half-edges.

Example 28. We continue Example 25. Figs. 6(e) and (c) show the NFG $\mathcal{N}_{\ker \partial_1}$ and the intermediate NFG used to obtain $\mathcal{N}_{\ker \partial_1}$ from \mathcal{N}_{∂_1} , respectively. Similarly, Figs. 6(i) and (g) show the NFG $\mathcal{N}_{\text{im } \partial_1}$ and the intermediate NFG used to obtain $\mathcal{N}_{\text{im } \partial_1}$ from \mathcal{N}_{∂_1} , respectively. ▽

We remark that the same subspace may be represented by many NFGs and so, besides the NFGs presented in this section, one can give several NFGs representing \mathcal{B}_{∂_1} , $\text{im } \partial_1$, and $\ker \partial_1$.

Another example where an NFG appeared whose exterior function is proportional to the indicator function of $\ker \partial_1$ is the support NFG of [19, Fig. 12]. In that paper, factor-graph representations of electrical networks are considered, and $\ker \partial_1$ appears naturally in that context because $\ker \partial_1$ encodes exactly Kirchhoff's current law when 1-chains are used to express currents along branches of an electrical network.⁹

In order to highlight the importance of NFGs whose exterior function is proportional to the indicator function of the kernel of some mapping, or proportional to the indicator function of the image of some mapping, let us connect the above findings to coding theory. Namely, in coding theory there are two popular approaches to define linear codes:

- In a *kernel representation*, a linear code of length n and dimension k over \mathbb{F} is described as the kernel of some linear map ϕ , i.e.,

$$\mathcal{C} \triangleq \{x \in \mathbb{F}^n \mid \phi(x) = 0\}.$$

Typically, the map ϕ is defined via a rank- $(n-k)$ parity-check matrix of size $m \times n$, where $m \geq n - k$. There are well-known approaches, in particular in the context

⁹Let us point out an important difference in the NFG drawing conventions used here and in [19]. Namely, whereas here arrows are used to label input and output half-edges, respectively, in the paper [19] arrows are used to express which arguments are taken positively and which arguments are taken negatively in a parity indicator function node.

of low-density parity-check codes, on how to specify an NFG whose exterior function is proportional to the indicator function of the code \mathcal{C} [5]–[7], [23], [24].

- In an *image representation*, a linear code of length n and dimension k over \mathbb{F} is described as the image of some linear map θ , i.e.,

$$\mathcal{C} \triangleq \{\theta(x) \mid x \in \mathbb{F}^k\}.$$

Typically, the map θ is defined via a generator matrix of size $k \times n$. Again, there are well-known approaches, in particular in the context of turbo and low-density generator-matrix codes on how to specify an NFG whose exterior function is proportional to the indicator function of the code \mathcal{C} [5]–[7].

Definition 29. In the following, an NFG whose support NFG equals $\mathcal{N}_{\text{im } \theta}$ for some linear mapping θ will be said to be in *image-representation form*. Similarly, an NFG whose support NFG equals $\mathcal{N}_{\ker \phi}$ for some linear mapping ϕ will be said to be in *kernel-representation form*. ■

We conclude this subsection by noting that besides introducing NFGs associated with the boundary operator ∂_1 , one can also introduce NFGs associated with the boundary operators ∂_2 and ∂_0 . The generalization of the above definitions is straightforward and we omit the details.

C. Cochains, coboundary operators, and cohomology spaces

For all the objects that we encountered in Section III-A, there are dual objects that we now introduce.

Definition 30. Given a 1-complex as in Definitions 16 and 21, for all $i = -1, 0, 1, 2$, let \widehat{C}_i be the dual space of C_i , i.e., the space of all linear maps from C_i to \mathbb{F} . Elements of \widehat{C}_i are called *i-cochains*. Note that $\widehat{C}_{-1} = \{0\}$ and $\widehat{C}_2 = \{0\}$. ■

Because \widehat{C}_0 is the dual space of C_0 , when defining an element φ of \widehat{C}_0 , we do not need to specify $\varphi(x)$ for all $x \in C_0$. It is sufficient to specify $\varphi(x)$ on any basis of C_0 , in particular, it is sufficient to specify $\varphi(x)$ for all $x \in \mathcal{V}$.

Definition 31. For all $i = 0, 1, 2$, we define the coboundary operator $d_i : \widehat{C}_{i-1} \rightarrow \widehat{C}_i$ to be the linear map which satisfies

$$(d_i \varphi)(\cdot) \triangleq \varphi(\partial_i(\cdot)) \quad \text{for all } \varphi \in \widehat{C}_{i-1}. \quad (27)$$

For $i = 1$, the condition in (27) implies the following for an arbitrary directed edge $a = (v, v')$ and an arbitrary $\varphi \in \widehat{C}_0$:

$$(d_1 \varphi)(a) = \varphi(\partial_1(a)) = \varphi(v' - v) = \varphi(v') - \varphi(v).$$

Therefore, $d_1 \varphi$ is the function that assigns to the directed edge a the difference between the φ -value at the ending vertex of the edge and the φ -value at the starting vertex of the edge.¹⁰

The objects that we have introduced in this subsection are summarized in (13); the collection of these objects is known as a 1-dimensional cochain complex.

¹⁰For example, in some physics application, φ might represent some potential function. Then $d_1 \varphi$ is the function that yields the potential differences along directed edges. We refer the interested reader to [2] for a very accessible introduction to the use of algebraic topology in physics.

Because d_0 and d_2 are the trivial maps, it holds that $\text{im } d_0 = \{0\}$ and $\ker d_2 = \widehat{C}_1$, from which it follows that

$$\text{im } d_0 \subseteq \ker d_1, \quad (28)$$

$$\text{im } d_1 \subseteq \ker d_2. \quad (29)$$

The fact that there might be a gap between $\text{im } d_0$ and $\ker d_1$ is captured by the 0-th cohomology space. Similarly, the fact that there might be a gap between $\text{im } d_1$ and $\ker d_2$ is captured by the 1-st cohomology space.

Definition 32. *The 0-th and the 1-st cohomology spaces are defined to be the quotient spaces*

$$\widehat{H}_0 \triangleq \ker d_1 / \text{im } d_0, \quad (30)$$

$$\widehat{H}_1 \triangleq \ker d_2 / \text{im } d_1, \quad (31)$$

respectively. \blacksquare

Again, although the relationships in (28) and (29) are rather trivial here, they will naturally generalize to m -complexes for $m \geq 2$.

Since (see Appendix A for details)

$$\ker d_i = (\text{im } \partial_i)^\perp, \quad (32)$$

$$\text{im } d_i = (\ker \partial_i)^\perp, \quad (33)$$

we have $\dim \widehat{H}_i = \dim H_i$ for $i = 0, 1$. Therefore, if one is interested in computing $\dim H_i$ for $i = 0, 1$, one can not only compute them via Definition 22, but also via $\dim H_i = \dim \widehat{H}_i$ and Definition 32.

D. NFG representation of the coboundary operator

In the same way that we associated the NFGs \mathcal{N}_{∂_1} , $\mathcal{N}_{\ker \partial_1}$, and $\mathcal{N}_{\text{im } \partial_1}$ with the linear map ∂_1 , we can associate the NFGs \mathcal{N}_{d_1} , $\mathcal{N}_{\ker d_1}$, and $\mathcal{N}_{\text{im } d_1}$ with the linear map d_1 .

We start by defining the set

$$\mathcal{B}_{d_1} \triangleq \{(\widehat{x}, \widehat{y}) \mid \widehat{x} \in \widehat{C}_0, \widehat{y} = d_1 \widehat{x}\},$$

which contains all possible pairs of a 0-cochain and its image under d_1 . In order to go from a coordinate-free representation of the elements of this set to a coordinate-based representation, we define bases for \widehat{C}_0 and \widehat{C}_1 such that the matrix representation of d_1 is the transpose of the matrix representation of ∂_1 . We can then write

$$\widehat{x} = \sum_{v \in \mathcal{V}} \widehat{x}(v) \cdot v,$$

$$d_1 \widehat{x} = \sum_{a \in \mathcal{A}} (d_1 \widehat{x})(a) \cdot a.$$

With this, we obtain

$$\mathcal{B}_{d_1} \triangleq \left\{ \left((\widehat{x}(v))_{v \in \mathcal{V}}, (\widehat{y}(a))_{a \in \mathcal{A}} \right) \mid \widehat{x} \in \widehat{C}_0, \widehat{y} = d_1 \widehat{x} \right\}.$$

The following definitions are analogous to Section III-D, and so we omit the details.

Definition 33. *Given a graph $\mathcal{G} = (\mathcal{V}, \mathcal{A})$, we define the input/output NFG \mathcal{N}_{d_1} associated with d_1 to be the NFG that has the following properties:*

- For every $a \in \mathcal{A}$, there is a parity indicator function with two full edges and an output (outgoing) half-edge whose associated variable is $\widehat{y}(a)$.
- For every $v \in \mathcal{V}$, there is an equality indicator function with a full edge (possibly with a sign inverter) for every edge incident on v and an input (ingoing) half-edge whose associated variable is $\widehat{x}(v)$.
- The full edges connect the indicator functions in the obvious way, i.e., the equality indicator function of $v \in \mathcal{V}$ is connected to the parity indicator function of $a \in \mathcal{A}$ iff a is incident on v . \blacksquare

Definition 34. *Given an input/output NFG \mathcal{N}_{d_1} , we define the NFG $\mathcal{N}_{\ker d_1}$ to be the NFG obtained from \mathcal{N}_{d_1} by deleting all the output half-edges. We also define $\mathcal{N}_{\text{im } d_1}$ as the NFG obtained from \mathcal{N}_{d_1} by deleting all the input-half edges. \blacksquare*

Example 35. *Consider again the graph $\mathcal{G} = (\mathcal{V}, \mathcal{A})$ in Fig. 4. Fig. 6(b) shows the input/output NFG \mathcal{N}_{d_1} ; Figs. 6(f) and (d) show the NFG $\mathcal{N}_{\ker d_1}$ and its intermediate version, respectively; Figs. 6(j) and (h) show the NFG $\mathcal{N}_{\text{im } d_1}$ and its intermediate version, respectively. \triangle*

From (32), (33), and (7) of Theorem 15, it is evident that, up to a scaling factor, we have

$$\mathcal{N}_{\text{im } d_1} = \widehat{\mathcal{N}}_{\ker \partial_1} \quad (34)$$

$$\mathcal{N}_{\ker d_1} = \widehat{\mathcal{N}}_{\text{im } \partial_1}. \quad (35)$$

(See Figs. 6(j) and (e), and Figs. 6(f) and (i), respectively.)

We conclude this subsection by noting that besides introducing NFGs associated with the coboundary operator d_1 , one can also introduce NFGs associated with the coboundary operators d_2 and d_0 .

IV. 2-COMPLEXES

The algebraic topology approach becomes more valuable when moving to 2-complexes, and, more generally, to higher-order complexes.

The present section is about 2-complexes and has a similar structure as Section III: in Section IV-A we introduce chains, boundary operators, and homology spaces, whereas in Section IV-C we introduce cochains, coboundary operators, and cohomology spaces; these sections are complemented by Sections IV-B and IV-D, where we introduce some NFGs that we associate with boundary and coboundary operators, respectively. Finally, because of the importance of 2-torus lattice graphs for later sections, Section IV-E discusses these objects in detail.

A. Chains, boundary operators, and homology spaces

Definition 36 (2-complex). *In addition to vertices and edges, a 2-complex also includes two-dimensional objects (surfaces). Consider a graph $\mathcal{G} \triangleq (\mathcal{V}, \mathcal{A})$ that can be drawn on some surface without edge crossings, then the graph divides the surface into regions called faces, which we denote by the set \mathcal{S} . In the following, we will use the notation $\mathcal{G} \triangleq (\mathcal{V}, \mathcal{A}, \mathcal{S})$ for such graphs. We define the following objects:*

- $C_0 \triangleq \mathbb{F}^{\mathcal{V}}$, whose elements are called 0-chains;

- $C_1 \triangleq \mathbb{F}^{\mathcal{A}}$, whose elements are called 1-chains.
- $C_2 \triangleq \mathbb{F}^{\mathcal{S}}$, whose elements are called 2-chains.

With a 0-chain $x \in \mathbb{F}^{\mathcal{V}}$, a 1-chain $y \in \mathbb{F}^{\mathcal{A}}$, a 2-chain $z \in \mathbb{F}^{\mathcal{S}}$ we associate the formal sums

$$x \triangleq \sum_{v \in \mathcal{V}} x(v) \cdot v, \quad y \triangleq \sum_{a \in \mathcal{A}} y(a) \cdot a, \quad z \triangleq \sum_{s \in \mathcal{S}} z(s) \cdot s,$$

respectively. \blacksquare

As in Section III, for every $a \in \mathcal{A}$ we fix a direction. Similarly, for every $s \in \mathcal{S}$, we fix an orientation. Namely, letting \mathcal{A}_s be the set of edges adjacent to the face s , we associate an orientation of s which refers to traversing the edges in \mathcal{A}_s in some direction (clockwise or counter-clockwise). The boundary of s is defined as the weighted sum of the edges in \mathcal{A}_s , where the weight of an edge depends on the relative direction of the edge w.r.t. to the chosen orientation of s .

Definition 37. The boundary operator $\partial_1 : C_1 \rightarrow C_0$, which maps 1-chains to 0-chains, is defined to be the (unique) linear map which satisfies

$$\text{for every } a = (v, v') \in \mathcal{A}: \quad \partial_1(a) \triangleq v' - v.$$

The boundary operator $\partial_2 : C_2 \rightarrow C_1$, which maps 2-chains to 1-chains, is defined to be the (unique) linear map which satisfies

$$\text{for every } s \in \mathcal{S}: \quad \partial_2(s) \triangleq \sum_{a \in \mathcal{A}_s} \alpha(a) \cdot a,$$

where \mathcal{A}_s is the set of edges adjacent to s and $\alpha(a) = +1$ if the direction of a is the same as the orientation of s (i.e., the direction in which \mathcal{A}_s is traversed) and $\alpha(a) = -1$ otherwise. \blacksquare

In the case of a planar graph, we take the orientation of an inner face to be clockwise and we take the orientation of the outer face, if it is included in \mathcal{S} , to be counter-clockwise.

Example 38. Consider the planar graph in Fig. 8(a) with $|\mathcal{V}| = 16$ vertices, $|\mathcal{A}| = 24$ edges, and $|\mathcal{S}| = 9$ faces. (Note that in this example there is no outer face.) In the following, we use a_{ij} to denote the directed edge (v_i, v_j) . We have

$$\begin{aligned} \partial_2 s_0 &= a_{01} + a_{15} - a_{45} - a_{04}, \\ \partial_2 s_1 &= a_{12} + a_{26} - a_{56} - a_{15}, \\ &\vdots = \vdots \quad \vdots \quad \vdots \quad \vdots \end{aligned}$$

Note that applying the boundary operator ∂_2 to $s_0 + s_1$ yields

$$\begin{aligned} \partial_2(s_0 + s_1) &= \partial_2(s_0) + \partial_2(s_1) \\ &= (a_{01} + a_{15} - a_{45} - a_{04}) + (a_{12} + a_{26} - a_{56} - a_{15}) \\ &= a_{01} + a_{12} + a_{26} - a_{56} - a_{45} - a_{04}. \end{aligned}$$

Example 39. The graph in Fig. 9(a) is similar to the graph in Fig. 8(a), but has only $|\mathcal{S}| = 8$ faces. Namely, the face s_4 has been removed, thereby leaving a ‘‘hole’’ in the plane. \triangle

The following definition turns out to be useful for subsequent considerations.

$$C_3 \xrightarrow{\partial_3} C_2 \xrightarrow{\partial_2} C_1 \xrightarrow{\partial_1} C_0 \xrightarrow{\partial_0} C_{-1} \quad (36)$$

$$\widehat{C}_3 \xleftarrow{d_3} \widehat{C}_2 \xleftarrow{d_2} \widehat{C}_1 \xleftarrow{d_1} \widehat{C}_0 \xleftarrow{d_0} \widehat{C}_{-1} \quad (37)$$

Fig. 7. Spaces and mappings associated with a 2-complex.

Definition 40. We define the sets $C_3 \triangleq \{0\}$ and $C_{-1} \triangleq \{0\}$, along with the trivial mappings $\partial_3 : C_3 \rightarrow C_2$ and $\partial_0 : C_0 \rightarrow C_{-1}$. \blacksquare

The objects that we have introduced so far are summarized in (36); the collection of these objects is known as a 2-dimensional chain complex, or simply 2-complex.

Note that the oriented boundary $\partial_2(s)$ of a face s is a cycle, i.e., it is in $\ker \partial_1$. Therefore, $\text{im } \partial_2 \subseteq \ker \partial_1$. This, together with the trivial observations $\text{im } \partial_3 = \{0\}$ and $\ker \partial_0 = C_0$ implies that

$$\text{im } \partial_3 \subseteq \ker \partial_2, \quad (38)$$

$$\text{im } \partial_2 \subseteq \ker \partial_1, \quad (39)$$

$$\text{im } \partial_1 \subseteq \ker \partial_0. \quad (40)$$

Definition 41. The 2-nd, the 1-st, and the 0-th homology spaces are defined to be the quotient spaces

$$H_2 \triangleq \ker \partial_2 / \text{im } \partial_3, \quad (41)$$

$$H_1 \triangleq \ker \partial_1 / \text{im } \partial_2, \quad (42)$$

$$H_0 \triangleq \ker \partial_0 / \text{im } \partial_1, \quad (43)$$

respectively. \blacksquare

Of particular interest is $\dim H_1$, which represents the number of ‘‘holes’’ of the 2-complex. Intuitively, the graph $\mathcal{G} = (\mathcal{V}, \mathcal{A}, \mathcal{S})$ in Fig. 8(a) has no hole, whereas the graph $\mathcal{G} = (\mathcal{V}, \mathcal{A}, \mathcal{S})$ in Fig. 9(a) has a hole because the latter graph is missing the surface element s_4 . This can be made more rigorous by considering closed curves that pass through the surface elements. In the case of Fig. 8(a), any such closed curve can be continuously contracted to a single point, whereas in the case of Fig. 9(a), this is not possible because of the missing surface element s_4 . (For more details, see, e.g., [3, Chap. 2].)

Example 42. We continue Example 38. Consider again the graph in Fig. 8(a). Similar to Example 23, the nine cycles $\partial_2 s_i$, $i = 0, 1, \dots, 8$, form a basis of $\ker \partial_1$, and so also form a basis of $\text{im } \partial_2 \subseteq \ker \partial_1$. Therefore,

$$\text{im } \partial_2 = \ker \partial_1, \quad (44)$$

which may equivalently be stated as

$$\dim H_1 = 0,$$

\triangle reflecting the lack of holes in this 2-complex.

We can compute $\dim H_2 = \dim(\ker \partial_2) - \dim(\text{im } \partial_3) = 0$ as follows. First, by the rank-nullity theorem, we have $\dim(\ker \partial_2) = 0$. Second, from the triviality of the map ∂_3 it follows that $\dim(\text{im } \partial_3) = 0$.

Finally, $\dim H_0$ equals the number of connected components of \mathcal{G} , which is one.

These findings can be summarized as follows:¹¹

$$\begin{array}{ccccc} & C_2 & \xrightarrow{\partial_2} & C_1 & \xrightarrow{\partial_1} & C_0 \\ \dim C_i & |S| & & |A| & & |V| \\ \dim H_i & 0 & & 0 & & 1, \end{array} \quad (45)$$

△

Remark 43. Equation (45) holds for any planar graph, provided that S is taken as the set of all inner faces. △

Remark 44. If we include the outer face, then we will have $\dim H_2 = 1$. To see this, note that adding the outer face will increase the dimension of C_2 by one, but leave the dimension of $\text{im } \partial_2$ unchanged since the boundary of the added face is contained in the original image space. (In our example, it is not hard to verify that the boundary of the outer face is equal to $-\partial_2(s_0 + s_1 + \dots + s_8)$.) Hence, as promised, we have $\dim(\ker \partial_2) = 1 = \dim H_2$, where the first equality is by the rank-nullity theorem and the second equality is by the triviality of ∂_3 . Finally, the dimensions of H_0 and H_1 remain unchanged. We summarize this as follows.

$$\begin{array}{ccccc} & C_2 & \xrightarrow{\partial_2} & C_1 & \xrightarrow{\partial_1} & C_0 \\ \dim C_i & |S| & & |A| & & |V| \\ \dim H_i & 1 & & 0 & & 1. \end{array} \quad (46)$$

△

Example 45. We continue Example 39. Consider again the graph in Fig. 9(a). Note that this 2-complex has 1-cycles that cannot be represented as the boundary of some 2-chains. For example, the cycle $a_{56} + a_{6,10} - a_{9,10} - a_{59}$ is such a 1-cycle. This points to the fact that, although the eight 1-cycles $\partial_2 s_i$, $i \in \{0, \dots, 8\} \setminus \{4\}$, form a basis of $\text{im } \partial_2$, they do not form a basis of $\ker \partial_1$. We would like to show that

$$\dim H_1 = 1,$$

which reflects the “hole” in the 2-complex represented by Fig. 9(a). This is indeed the case since, starting with the faces as in Example 42, then removing s_4 does not affect $\ker \partial_1$, but it reduces $\dim(\text{im } \partial_2)$ by one, since $\partial_2(s_i)$, $i = 0, \dots, 8$, are independent as observed in Example 42.

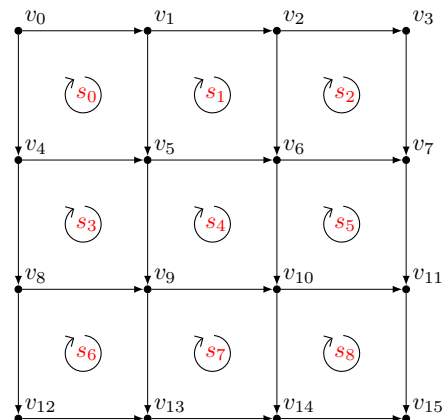
For $\dim H_2$ and $\dim H_0$ we obtain 0 and 1, respectively. Overall, these findings can be summarized as follows:

$$\begin{array}{ccccc} & C_2 & \xrightarrow{\partial_2} & C_1 & \xrightarrow{\partial_1} & C_0 \\ \dim C_i & |S| & & |A| & & |V| \\ \dim H_i & 0 & & 1 & & 1 \end{array} \quad (47)$$

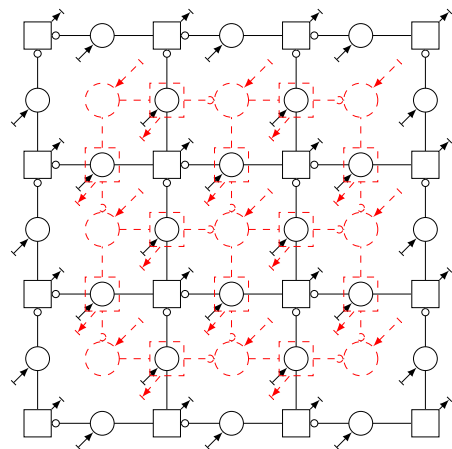
△

Let us conclude this section by pointing out that there are quantum stabilizer codes based on 2-complexes. For these codes, the number of information qubits equals $\dim H_1$. We refer the interested reader to [25] about the so-called toric (quantum stabilizer) code. See also the discussion in [14].

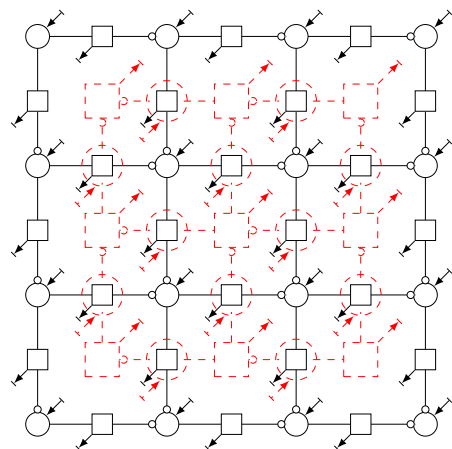
¹¹Here and in the following, we omit the trivial spaces C_3 and C_{-1} when discussing 2-complexes.



(a) Graph $\mathcal{G} = (\mathcal{V}, \mathcal{A}, \mathcal{S})$



(b) NFG \mathcal{N}_{∂_1} (black, solid) and NFG \mathcal{N}_{∂_2} (red, dashed)



(c) NFG \mathcal{N}_{∂_1} (black, solid) and NFG \mathcal{N}_{∂_2} (red, dashed)

Fig. 8. A graph $\mathcal{G} = (\mathcal{V}, \mathcal{A}, \mathcal{S})$ and associated NFGs. To allow a clearer overlay of figures, we deviate from conventions here and use a circle node to denote an equality indicator function and a square node to denote a parity indicator function.

B. NFG representation of the boundary operator

It is straightforward to generalize the definitions in Section III-B to 2-complexes. In this subsection, we will therefore only discuss some examples.

Example 46. We continue Examples 38 and 42. Fig. 8(b)

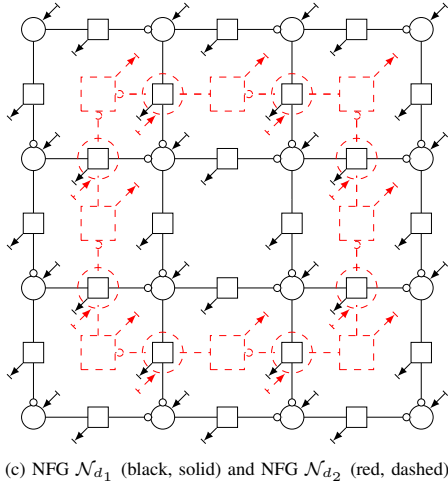
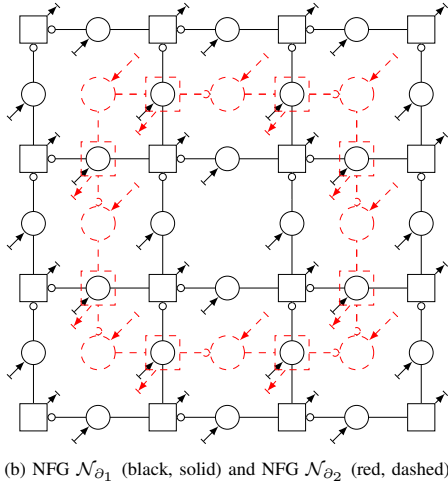
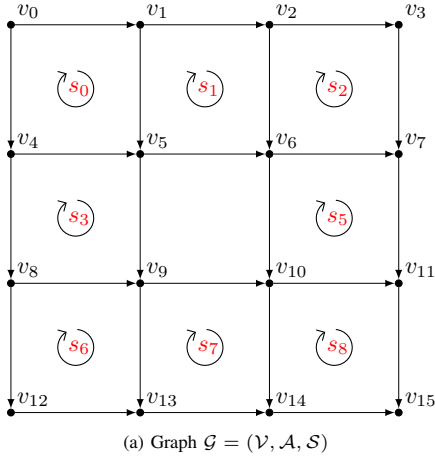


Fig. 9. A graph $\mathcal{G} = (\mathcal{V}, \mathcal{A}, \mathcal{S})$ and associated NFGs. To allow a clearer overlay of figures, we deviate from conventions here and use a circle node to denote an equality indicator function and a square node to denote a parity indicator function.

shows an input/output NFG \mathcal{N}_{∂_1} (black, solid lines) and an input/output NFG \mathcal{N}_{∂_2} (red, dashed lines). To allow a clearer overlay of NFGs in this figure, we omit the “=” and “+” symbols and draw an equality indicator function as a circle node and a parity indicator function as a square node. Note

that the output half-edges of \mathcal{N}_{∂_2} are in parallel to the input half-edges of \mathcal{N}_{∂_1} . If we remove such pairs of half-edges and replace them by full-edges connecting \mathcal{N}_{∂_2} and \mathcal{N}_{∂_1} , we obtain the input/output NFG $\mathcal{N}_{\partial_1 \circ \partial_2}$ corresponding to the mapping $\partial_1 \circ \partial_2$, which is the concatenation of first applying the mapping ∂_2 and then the mapping ∂_1 . Note that because $\partial_1 \circ \partial_2 = 0$, which is a consequence of $\text{im } \partial_2 \subseteq \ker \partial_1$, this mapping is trivial. \triangle

Example 47. We continue Examples 39 and 45. Fig. 9(b) shows an input/output NFG \mathcal{N}_{∂_1} (black, solid lines) and an input/output NFG \mathcal{N}_{∂_2} (red, dashed lines). \triangle

It should be clear that once we have drawn \mathcal{N}_μ for some linear mapping μ , we can easily obtain $\mathcal{N}_{\ker \mu}$ and $\mathcal{N}_{\text{im } \mu}$.

C. Cochains, coboundary operators, and cohomology spaces

For all the objects that we encountered in Section IV-A, there are dual objects that we now introduce.

Definition 48. Given a 2-complex as in Definitions 36 and 40, for all $i = -1, 0, 1, 2, 3$, let \widehat{C}_i be the dual space of C_i , i.e., the space of all linear maps from C_i to \mathbb{F} . Elements of \widehat{C}_i are called i -cochains. Note that $\widehat{C}_{-1} = \{0\}$ and $\widehat{C}_3 = \{0\}$. \blacksquare

For $i = 0, 1, 2, 3$, the coboundary operator d_i is defined analogously to Definition 31. For $i = 2$, the condition in (27) implies the following for an arbitrary face $s \in \mathcal{S}$ and an arbitrary $\varphi \in \widehat{C}_1$:

$$(d_2\varphi)(s) = \varphi(\partial_2(s)) = \varphi\left(\sum_{a \in A_s} \alpha(a) \cdot a\right) = \sum_{a \in A_s} \alpha(a) \cdot \varphi(a),$$

where we have used the notation as in Definition 37. If φ represents some flow along the directed edges, then $d_2\varphi$ is the function that yields the curl around oriented faces.

Note that if a flow is obtained by applying the coboundary operator d_1 to a 0-chain representing some potential function, then the curl around any oriented face will be zero. This implies that $\text{im } d_1 \subseteq \ker d_2$. (This generalizes a well-known result from vector calculus which states that $\text{curl} \circ \text{grad} = 0$. See [2, Section 15.4] for a more general discussion.) Because $\text{im } d_0 = \{0\}$ and $\ker d_3 = \widehat{C}_2$, we therefore have

$$\text{im } d_0 \subseteq \ker d_1, \quad (48)$$

$$\text{im } d_1 \subseteq \ker d_2, \quad (49)$$

$$\text{im } d_2 \subseteq \ker d_3. \quad (50)$$

The fact that there might be a gap between $\text{im } d_i$ and $\ker d_{i+1}$, $i = 0, 1, 2$, is captured by the i -th cohomology space.

Definition 49. The 0-th, the 1-st, and the 2-nd cohomology spaces are defined to be the quotient spaces

$$\widehat{H}_0 \triangleq \ker d_1 / \text{im } d_0, \quad (51)$$

$$\widehat{H}_1 \triangleq \ker d_2 / \text{im } d_1, \quad (52)$$

$$\widehat{H}_2 \triangleq \ker d_3 / \text{im } d_2, \quad (53)$$

respectively. \blacksquare

A similar argument to the one in Section III-C gives $\dim \widehat{H}_i = \dim H_i$ for $i = 0, 1, 2$, and so, $\dim \widehat{H}_i$ has the same interpretation as $\dim H_i$.

The objects that we have introduced in this subsection are summarized in (37); the collection of these objects is known as a 2-dimensional cochain complex.

An important application of these homology and cohomology spaces is to characterize continuous 2-dimensional surfaces. This can be done by triangulating these surfaces and studying the dimension of the resulting homology and cohomology spaces. Most importantly, for a given i , $\dim H_i$ will be independent of the chosen triangulation.

D. NFG representation of the coboundary operator

It is straightforward to generalize the definitions in Section III-D to 2-complexes. In this subsection, we will therefore only discuss some examples.

Example 50. We continue Examples 38, 42, and 46. Fig. 8(c) shows an input/output NFG \mathcal{N}_{d_1} (black, solid lines) and an input/output NFG \mathcal{N}_{d_2} (red, dashed lines). Note that the output half-edges of \mathcal{N}_{d_1} are in parallel to the input half-edges of \mathcal{N}_{d_2} . If we remove such pairs of half-edges and replace them by full-edges connecting \mathcal{N}_{d_1} and \mathcal{N}_{d_2} , we obtain the input/output NFG $\mathcal{N}_{d_2 \circ d_1}$ corresponding to the mapping $d_2 \circ d_1$. Note that because $d_2 \circ d_1 = 0$, which is a consequence of $\text{im } d_1 \subseteq \ker d_2$, this mapping is trivial. \triangle

Example 51. We continue Examples 39, 45, and 47. Fig. 9(c) shows an input/output NFG \mathcal{N}_{d_1} (black, solid lines) and an input/output NFG \mathcal{N}_{d_2} (red, dashed lines). \triangle

We conclude this subsection by noting that an example where an NFG appeared whose exterior function is proportional to $\text{im } d_1$ is the support NFG of Fig. 11 in [19]. In that paper, factor-graph representations of electrical networks are considered, and $\ker d_2$ and $\text{im } d_1$ appear naturally in that context because $\ker d_2$ encodes exactly Kirchhoff's voltage law and $\text{im } d_1$ gives voltage differences along edges based on voltage potentials at nodes. Because $\text{im } d_1 \subseteq \ker d_2$, these voltage differences automatically satisfy Kirchhoff's voltage law.

E. 2-torus lattice graph

Because of the importance of 2-torus lattice graphs for later sections, this subsection discusses this object in detail.

We define a 2-torus lattice graph as a 2-dimensional square lattice graph drawn on a torus. Namely, the graph \mathcal{G} in Fig. 10(a) is a 2-torus lattice graph, which is obtained from the graph in Fig. 4 by identifying the left and right most edges (resulting in a cylinder) and the top and bottom most edges (resulting in a doughnut shape). More explicitly, the graph $\mathcal{G} \triangleq (\mathcal{V}, \mathcal{A}, \mathcal{S})$ in Fig. 10(a) is obtained from the graph in Fig. 4 as follows:

- v_0 is obtained by identifying v_0, v_2, v_6, v_8 ;
- v_1 is obtained by identifying v_1, v_7 ;
- v_2 is obtained by identifying v_3, v_5 ;
- v_3 is obtained from v_4 ;

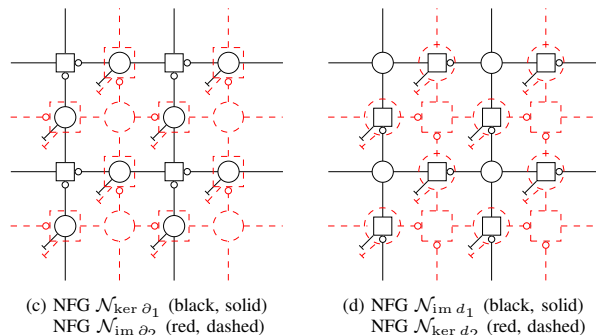
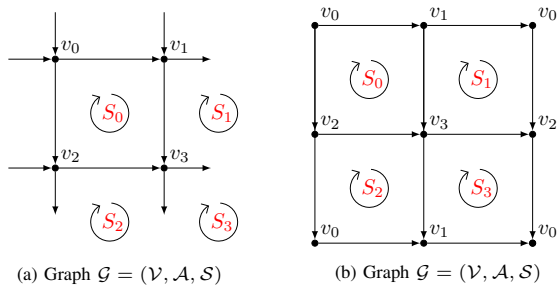


Fig. 10. A 2-torus lattice graph $\mathcal{G} = (\mathcal{V}, \mathcal{A}, \mathcal{S})$ and its associated NFGs. To allow a clearer overlay of figures, we deviate from conventions here and use a circle node to denote an equality indicator function and a square node to denote a parity indicator function. In (c) and (d) the left and right most edges are identified and the top and bottom most edges are identified.

- edges in Fig. 10(a) are obtained by identifying edges in Fig. 4 in a manner consistent with the above vertex identifications.

In other words, the resulting graph in Fig. 10(a) is such that the edge in Fig. 10(a) that leaves v_2 downwards continues as the edge that enters v_0 from above, etc. Note that $|\mathcal{V}| = 4$, $|\mathcal{A}| = 8$, and $|\mathcal{S}| = 4$.

An alternative representation of the graph in Fig. 10(a) is shown in Fig. 10(b), where identically labeled vertices and edges are identified.

Figs. 10(c) and (d) show some of the NFGs that can be associated with the graph in Fig. 10(a).

Lemma 52. For the above-defined 2-torus lattice graph it holds that

$$\dim H_1 = 2.$$

Proof. We first show that $\dim(\ker \partial_1) = 5$ and that $\dim(\text{im } \partial_2) = 3$. This then yields

$$\begin{aligned} \dim H_1 &= \dim(\ker \partial_1 / \text{im } \partial_2) \\ &= \dim(\ker \partial_1) - \dim(\text{im } \partial_2) \\ &= 5 - 3 \\ &= 2, \end{aligned}$$

which is the promised result. The result $\dim(\ker \partial_1) = 5$ follows immediately from (20) as $\dim(\ker \partial_1) = |\mathcal{A}| - (|\mathcal{V}| - 1) = 5$. On the other hand, the result $\dim(\text{im } \partial_2) = 3$ follows

from observing that the boundary of a 2-chain is equal to zero if and only if it is (up to a scaling factor in \mathbb{F}) equal to the sum of all the faces, i.e., $\dim(\ker \partial_2) = 1$. Therefore, $\dim(\text{im } \partial_2) = |\mathcal{S}| - 1 = 3$. \square

The fact that $\dim H_1 > 0$ is an indication that the graph $\mathcal{G} \triangleq (\mathcal{V}, \mathcal{A}, \mathcal{S})$ has holes, i.e., there are cycles in C_1 that cannot be written as boundaries of 2-chains. The space H_1 consists of the equivalence classes of such cycles, where two cycles are equivalent if they differ by a boundary of a 2-chain. Because $\dim H_1 = 2$, a basis of H_1 consists of two such equivalence classes.

Let $\{c_h + \text{im } \partial_2, c_v + \text{im } \partial_2\}$ be a basis of H_1 , where $c_h, c_v \in \ker \partial_1 \setminus \text{im } \partial_2$ are two non-equivalent cycles that are not boundaries, say,

$$\begin{aligned} c_h &\triangleq a_{01} + a_{10}, \\ c_v &\triangleq a_{02} + a_{20}. \end{aligned}$$

(Here ‘‘h’’ and ‘‘v’’ stand for ‘‘horizontal’’ and ‘‘vertical’’ w.r.t. Figs. 10(a) or (b).) Then one can express the space of 1-cycles as the union of the cosets

$$\ker \partial_1 = \bigcup_{\alpha_h, \alpha_v \in \mathbb{F}} (\alpha_h \cdot c_h + \alpha_v \cdot c_v + \text{im } \partial_2).$$

Fig. 10(c) shows the NFGs representing $\text{im } \partial_2$ (dashed) and $\ker \partial_1$ (solid).

The above findings can easily be generalized to the 2-torus lattice graph with $n \triangleq L_1 \times L_2$ vertices, where L_1 and L_2 are arbitrary integers larger than one. (This 2-torus lattice graph can be obtained from the $(L_1 + 1) \times (L_2 + 1)$ square lattice using a similar identification of edges and vertices as described at the beginning of the subsection.) In particular, we find that $\dim(\text{im } \partial_2) = n - 1$ and $\dim(\ker \partial_1) = n + 1$, which imply $\dim H_1 = 2$ for all L_1 and all L_2 . Moreover, using the obvious extension of the vertices’ indexing, i.e., by indexing the first row of vertices by $0, \dots, L_2 - 1$, the second row by $L_2, \dots, 2L_2 - 1$, etc., one may choose

$$\begin{aligned} c_h &= a_{0,1} + a_{1,2} + \dots + a_{L_2-1,0}, \\ c_v &= a_{0,L_2} + a_{L_2,2L_2} + \dots + a_{(L_1-1)L_2,0}, \end{aligned}$$

such that

$$\ker \partial_1 = \bigcup_{\alpha_h, \alpha_v \in \mathbb{F}} (\alpha_h \cdot c_h + \alpha_v \cdot c_v + \text{im } \partial_2). \quad (54)$$

Finally, since $\dim H_0 = 1$ for a connected graph and $\dim H_2 = \dim(\ker \partial_2)$ for a 2-complex, we may summarize our discussion of the 2-torus lattice graph by

$$\begin{array}{ccccc} C_2 & \xrightarrow{\partial_2} & C_1 & \xrightarrow{\partial_1} & C_0 \\ \dim C_i & n & 2n & n & \\ \dim H_i & 1 & 2 & 1. & \end{array} \quad (55)$$

We conclude this section with the following observation that will be useful in Section VI-C. Namely, for the 2-torus lattice graph, we have

$$\text{im } \partial_2 = \text{im } d_1. \quad (56)$$

This can be seen by comparing Figs. 10(c) (red, dashed lines) and (d) (black, solid lines), and is a consequence of

the *self-duality* of the 2-torus lattice graph. Namely, for any graph $\mathcal{G} = (\mathcal{V}, \mathcal{A}, \mathcal{S})$ the *dual graph* $\mathcal{G}_d \triangleq (\mathcal{S}, \mathcal{A}_d, \mathcal{V})$ is defined such that any two vertices in \mathcal{G}_d are adjacent iff the corresponding surfaces in \mathcal{G} share an edge. (One can properly define directions for the edges, but we omit the details.) With this definition, one can verify that the graph \mathcal{G} in Fig. 10(a) is isomorphic to its dual, which consequently leads to (56).

We conclude this section on 2-complexes by pointing out Appendix A on higher-order complexes.

V. STATISTICAL MODELS

In this section we offer a brief introduction to statistical models, in particular to the Boltzmann distribution and the partition function.

A *statistical model* is defined as a collection of random variables (RVs) $\{X_1, \dots, X_n\}$, where each RV assumes values from a finite set \mathcal{X} . (Frequently, X_1, \dots, X_n are called spins.) With each configuration $x \in \mathcal{X}^n$ we associate an energy level $E(x)$ such that the joint distribution of the RVs is the Boltzmann distribution

$$p(x) \triangleq \frac{e^{-\beta E(x)}}{Z}, \quad (57)$$

where Z is the partition function defined as

$$Z \triangleq \sum_{x \in \mathcal{X}^n} e^{-\beta E(x)},$$

where $\beta \triangleq \frac{1}{kT}$ is the inverse temperature, and where k and T are, respectively, the Boltzmann constant and the temperature.

At first sight, Z is ‘‘only’’ a temperature-dependent normalization constant that appears in (57). However, the way Z changes with temperature T (and more generally with other parameters like pressure) tells a lot about how macroscopic properties of a system change with changing temperature. In particular, in the limit $n \rightarrow \infty$ (the so-called thermodynamic limit), Z or its derivatives might exhibit discontinuities, thereby delineating phase transitions [26].

Note that the partition function not only appears in statistical physics in the study of macroscopic properties induced by the microscopic properties, but, among other areas, also in the following fundamental problems:

- the capacity of a constrained channel in information theory (see, e.g., [27]),
- the number of graph (vertex) colorings in graph theory (see, e.g., [28]),
- permanents, graph homomorphism, integer flows, etc. (see, e.g., [29]).

Given the importance of the partition function in various fields, several approaches have been devised to tackle the partition function from different angles. This has resulted in a variety of methods that have provided:

- estimates of the partition function, e.g., stochastic approximations [30], the renormalization group approximation [31], [32], and the Bethe approximation [33];
- bounds on the partition function [34];
- identities that the partition function satisfies, such as the Kramers–Wannier duality [9].

A central topic of the remaining sections will be the re-derivation of the Kramers–Wannier duality for the two-dimensional Ising model with the help of NFGs and the concepts introduced in earlier sections. The use of some notions from algebraic topology toward proving the Kramers–Wannier duality is not new [10], [11], however, the separation of the arguments leading to the Kramers–Wannier duality into two steps, as discussed below, seems natural, and concisely points out what is needed for a Kramers–Wannier-type duality to hold. (See also Fig. 13.) Moreover, Kramers–Wannier duality is typically argued in the limit when the size of the square lattice (on the torus) is large. In contrast, the results provided here hold for any size of the lattice.

VI. KRAMERS–WANNIER DUALITY FOR THE ISING MODEL

In this section we first introduce the Ising model. Afterwards, we suitably combine the results that we have encountered in earlier sections toward re-deriving the Kramers–Wannier duality for that model.

A. Ising model

Let L be an arbitrary positive integer and define $n \triangleq L^2$. The Ising model [12] (see, e.g., [26]) is a statistical model with binary spins, where, w.l.o.g., we will assume $\mathcal{X} \triangleq \mathbb{F}_2$. Moreover, the spins are arranged over some lattice vertices (called sites). The two-dimensional nearest-neighbor (ferromagnetic) Ising model is one where the lattice is chosen as the square lattice of size $L \times L$ (on the plane or the torus), and the energy of a configuration $x \in \mathbb{F}_2^n$ is defined as

$$E(x) \triangleq - \sum_{(i,j) \in \mathcal{A}} (2\delta_{=}(x_i, x_j) - 1), \quad (58)$$

where \mathcal{A} is the set of edges of the lattice.¹² Subsequently, unless specified otherwise, we will refer to this model simply as the (two-dimensional) Ising model. In this case, the partition function can be written as

$$Z = \sum_{x \in \mathbb{F}_2^n} \prod_{(i,j) \in \mathcal{A}} \kappa_\beta(x_j - x_i), \quad (59)$$

where

$$\begin{aligned} \kappa_\beta(0) &\triangleq e^\beta, \\ \kappa_\beta(1) &\triangleq e^{-\beta}. \end{aligned} \quad (60)$$

If β is clear from the context, then we will simply write κ instead of κ_β .

Rewriting the r.h.s. of (59) more explicitly as

$$\sum_{x \in \mathbb{F}_2^n} \sum_{x \in \mathbb{F}_2^{2n}} \prod_{e \in \mathcal{A}} \kappa_\beta(x_e) \cdot \delta_+(x_e, x_i, -x_j), \quad (61)$$

it is clear that

$$Z = Z_{\mathcal{N}_{\text{I}(\beta)}}, \quad (62)$$

¹²The convention taken by physicists in adopting the minus sign in (58) is so that the configurations with aligned spins (i.e., the configurations where all spins are equal) have the lowest energy level.

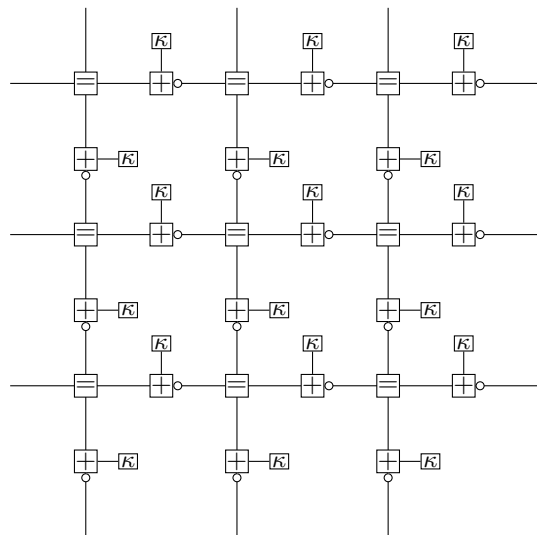


Fig. 11. The NFG $\mathcal{N}_{\text{I}(\beta)}$ representing the Ising model on the torus. (Note: the leftmost edges are identified with the rightmost edges and the topmost edges are identified with the bottommost edges. Moreover, κ is shorthand notation for κ_β .)

where $\mathcal{N}_{\text{I}(\beta)}$ is the pairwise interaction NFG in Fig. 11 (see Definition 8). In other words, the NFG $\mathcal{N}_{\text{I}(\beta)}$ represents the Ising model on the torus at inverse temperature β , where, as was discussed in Section II-B, the sites are represented by equality indicator functions and the parity indicator functions ensure that the interaction between a pair of adjacent sites depends only on the difference (modulo 2) between their spins. From (62), and by recalling the definition of $\mathcal{C}_{\mathcal{N}}$ from (1), we note that (59) can also be written as

$$Z = 2 \cdot \sum_{x \in \mathcal{C}_{\mathcal{N}_{\text{I}(\beta)}}} \prod_{e \in \mathcal{A}} \kappa_\beta(x_e). \quad (63)$$

The factor 2 stems from the fact that for every term in the sum $\sum_{x \in \mathcal{C}_{\mathcal{N}_{\text{I}(\beta)}}} \cdots$ in (63) there are $|\mathbb{F}_2| = 2$ corresponding terms in the sum $\sum_{x \in \mathbb{F}_2^n} \cdots$ in (59).

B. Fourier-transformed NFG of Ising model

In the previous subsection we saw that the NFG $\mathcal{N}_{\text{I}(\beta)}$ represents the partition function of the Ising model. From Section II-C, another obvious NFG that represents the partition function of the Ising model is the Fourier-transformed NFG $\widehat{\mathcal{N}}_{\text{I}(\beta)}$ in Fig. 12. Namely, we have

$$Z \stackrel{(62)}{=} Z_{\mathcal{N}_{\text{I}(\beta)}} = 2^{-n} Z_{\widehat{\mathcal{N}}_{\text{I}(\beta)}}, \quad (64)$$

where the second equality is by (8) of Theorem 15 upon noting that $|\mathcal{A}| - |\mathcal{V}| = n$ for the torus. This expression of the partition function can be written more explicitly as

$$Z = 2^{-n} \sum_{x \in \mathcal{C}_{\widehat{\mathcal{N}}_{\text{I}(\beta)}}} \prod_{e \in \mathcal{A}} \widehat{\kappa}_\beta(x_e).$$

We now make the following observations about $\widehat{\mathcal{N}}_{\text{I}(\beta)}$.

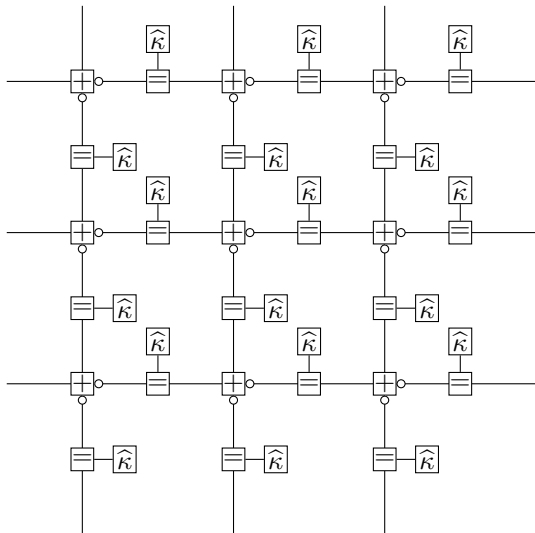


Fig. 12. The Fourier-transformed NFG $\widehat{\mathcal{N}}_{I(\beta)}$. (Note: the leftmost edges are identified with the rightmost edges and the topmost edges are identified with the bottommost edges. $\widehat{\kappa}$ is shorthand notation for $\widehat{\kappa}_\beta$.)

- A degree-one function in $\widehat{\mathcal{N}}_{I(\beta)}$ is the Fourier transform

$$\begin{aligned}\widehat{\kappa}_\beta(0) &= e^\beta + e^{-\beta}, \\ \widehat{\kappa}_\beta(1) &= e^\beta - e^{-\beta}\end{aligned}\quad (65)$$

of κ_β . Note that at large β , i.e., low temperature, we have $\kappa_\beta(0) \gg \kappa_\beta(1)$. Consequently, the function $\prod_e \kappa_\beta(x_e)$, which is defined on a high-dimensional space, is strongly irregular, i.e., it contains high peaks and deep valleys, making it harder for sampling-based methods to provide an accurate estimate of the partition function.

In contrast, the Fourier transform shows the opposite trend. Namely, at low temperature, we have $\widehat{\kappa}_\beta(0) \approx \widehat{\kappa}_\beta(1)$. Consequently, the function $\prod_e \widehat{\kappa}_\beta(x_e)$, which is also defined on a high-dimensional space, is almost flat, making it easier for sampling-based methods to provide an accurate estimate of the partition function.

This observation is reversed at small values of β , i.e., high temperature, where sampling estimators based on the interaction NFG $\mathcal{N}_{I(\beta)}$ outperform estimators based on the Fourier-transformed NFG $\widehat{\mathcal{N}}_{I(\beta)}$. For more details, we refer the reader to [35]–[37].

- The above trend carries on beyond the Ising model [37]. However, in the case of the Ising model one can make the above argument more explicit. Namely, from (60) and (65), we can write $\widehat{\kappa}_\beta$ as

$$\widehat{\kappa}_\beta(x) = \sqrt{2 \cdot c_\beta} \cdot \kappa_\beta(x), \quad \forall x \in \mathbb{F}_2, \quad (66)$$

where

$$c_\beta \triangleq 2 \cdot \sinh(\beta) \cdot \cosh(\beta) \quad (67)$$

and the dual inverse temperature $\widetilde{\beta}$ is defined as

$$\widetilde{\beta} \triangleq -\frac{1}{2} \log(\tanh \beta). \quad (68)$$

Note that c_β does not depend on x and so can be carried outside the summation when computing the partition function. Moreover, the dual inverse temperature is a strictly decreasing function of β , i.e., the function $-\frac{1}{2} \log(\tanh(\cdot))$ maps high temperatures to low temperatures, and vice versa.

- Although the Fourier transform maps low temperatures to high temperatures, the resulting NFG $\widehat{\mathcal{N}}_{I(\beta)}$, unlike $\mathcal{N}_{I(\beta)}$, is not a pairwise interaction NFG (see Definition 8). The task of mapping $\widehat{\mathcal{N}}_{I(\beta)}$ to a pairwise interaction NFG at high temperature will be discussed in the next subsection. (Even though this last step, i.e., from $\widehat{\mathcal{N}}_{I(\beta)}$ to a pairwise interaction NFG at high temperature, may not be required if one is interested in sampling-based approaches for estimating the partition function, from a theoretical perspective it can lead to very valuable insights.)

C. Kramers–Wannier duality

Consider an Ising model on the torus, which can be represented by an NFG $\mathcal{N}_{I(\beta)}$ as in Fig. 11. Kramers and Wannier [9] (see also [10], [11]) made the observation that the partition function of the Ising model at inverse temperature β can be expressed in terms of the partition function of the Ising model at the dual inverse temperature $\widetilde{\beta}$ defined in (68).

More precisely, one can make the following statement.

Theorem 53. *For the Ising model on the 2-torus lattice graph of size n , we have*

$$\lim_{n \rightarrow \infty} \frac{1}{n} \log(Z_{\mathcal{N}_{I(\beta)}}) = \log(c_\beta) + \lim_{n \rightarrow \infty} \frac{1}{n} \log(Z_{\mathcal{N}_{I(\widetilde{\beta})}}), \quad (69)$$

where c_β and $\widetilde{\beta}$ were defined in (67) and (68), respectively. ■

Our approach to proving the above result consists of first proving a more general result that holds for finite n and then to take the limit $n \rightarrow \infty$.

Recall the definition of the cycles c_h and c_v in Section IV-E. In order to state our result, we use the following notation. For any real number $\alpha \geq 0$, we define $\mathcal{N}_{I(\alpha)}^h$ to be the same NFG as $\mathcal{N}_{I(\alpha)}$ but with the interaction function

$$\kappa_\alpha(\cdot) \text{ replaced by } \kappa_\alpha(1 - \cdot)$$

along the cycle c_h . We similarly define $\mathcal{N}_{I(\alpha)}^v$, where the replacement is made along the cycle c_v ; and $\mathcal{N}_{I(\alpha)}^{hv}$, where the replacement is made along both c_h and c_v .

Theorem 54. *For the Ising model on the 2-torus lattice graph of size n , we have*

$$Z_{\mathcal{N}_{I(\beta)}} = \frac{c_\beta^n}{2} \cdot \left(Z_{\mathcal{N}_{I(\widetilde{\beta})}} + Z_{\mathcal{N}_{I(\widetilde{\beta})}^h} + Z_{\mathcal{N}_{I(\widetilde{\beta})}^v} + Z_{\mathcal{N}_{I(\widetilde{\beta})}^{hv}} \right), \quad (70)$$

where c_β and $\widetilde{\beta}$ were defined in (67) and (68), respectively. ■

Proof. First note that

$$\mathcal{C}_{\mathcal{N}_{I(\beta)}} = \text{im } d_1, \quad (71)$$

which is clear by comparing the support NFG of $\mathcal{N}_{I(\beta)}$ in Fig. 11 and Fig. 10(d) (black, solid lines). We prove the theorem in two steps, namely, we separately show that

$$Z_{\mathcal{N}_{I(\beta)}} = 2^{-n} \cdot Z_{\widehat{\mathcal{N}}_{I(\beta)}}, \quad (72)$$

$$Z_{\widehat{\mathcal{N}}_{I(\beta)}} = 2^{n-1} \cdot c_\beta^n \cdot (Z_{\mathcal{N}_{I(\tilde{\beta})}} + Z_{\mathcal{N}_{I(\tilde{\beta})}^h} + Z_{\mathcal{N}_{I(\tilde{\beta})}^v} + Z_{\mathcal{N}_{I(\tilde{\beta})}^{hv}}). \quad (73)$$

The expression in (72) follows from (8) of Theorem 15 upon noting that $|\mathcal{A}| - |\mathcal{V}| = n$ for the 2-torus lattice graph.

The expression in (73) can be shown as follows. Namely,

$$\begin{aligned} & Z_{\widehat{\mathcal{N}}_{I(\beta)}} \\ & \stackrel{(i)}{=} \sum_{x \in \ker \partial_1} \prod_{e \in \mathcal{A}} \widehat{\kappa}_\beta(x_e) \\ & \stackrel{(ii)}{=} \sum_{x \in \text{im } \partial_2} \prod_{e \in \mathcal{A}} \widehat{\kappa}_\beta(x_e) + \cdots + \sum_{x \in c_v + c_h + \text{im } \partial_2} \prod_{e \in \mathcal{A}} \widehat{\kappa}_\beta(x_e) \\ & = \sum_{x \in \text{im } \partial_2} \prod_{e \in \mathcal{A}} \widehat{\kappa}_\beta(x_e) + \cdots + \sum_{x \in \text{im } \partial_2} \prod_{e \in \mathcal{A}} \widehat{\kappa}_\beta(x_e + c_v + c_h) \\ & \stackrel{(iii)}{=} (\sqrt{2c_\beta})^{2n} \cdot \left(\sum_{x \in \text{im } \partial_2} \prod_{e \in \mathcal{A}} \kappa_{\tilde{\beta}}(x_e) + \cdots \right) \\ & \stackrel{(iv)}{=} 2^n c_\beta^n \cdot \left(\sum_{x \in \mathcal{C}_{\mathcal{N}_{I(\tilde{\beta})}}} \prod_{(i,j) \in \mathcal{A}} \kappa_{\tilde{\beta}}(x_j - x_i) + \cdots \right) \\ & \stackrel{(v)}{=} 2^{n-1} \cdot c_\beta^n \cdot (Z_{\mathcal{N}_{I(\tilde{\beta})}} + \cdots), \end{aligned}$$

where equality (i) follows from (71) and (35), equality (ii) follows from (54), equality (iii) follows from expressing $\widehat{\kappa}_\beta$ in terms of $\kappa_{\tilde{\beta}}$ (see (66)–(68)), equality (iv) follows from the self-duality of the 2-torus lattice graph (56) and (71), and equality (v) follows from (63) and the fact that the support NFG is independent of β , i.e., $\mathcal{C}_{\mathcal{N}_{I(\beta)}} = \mathcal{C}_{\mathcal{N}_{I(\tilde{\beta})}}$. \square

Here we also give a summary of the proof using Figs. 10(c) and (d). The NFG $\mathcal{N}_{I(\beta)}$ is in image representation since its support NFG is equal to $\mathcal{N}_{\text{im } \partial_1}$, as can be seen by comparing Fig. 11 and Fig. 10(d) (black, solid lines). The NFG $\widehat{\mathcal{N}}_{I(\beta)}$ is in kernel representation since its support NFG is equal to $\mathcal{N}_{\ker \partial_1}$, as can be seen by comparing Fig. 12 and Fig. 10(c) (black, solid lines). Note that in Fig. 10, the NFGs in image-representation form are pairwise interaction NFGs, while the NFGs in kernel-representation form are not pairwise interaction NFGs. The purpose of (72) is to invert the temperature, which is accomplished via the Fourier transform. As a side effect, the image representation form (pairwise interaction) is lost since this step causes $\mathcal{N}_{\text{im } \partial_1}$ (Fig. 10(d) black, solid lines) to be replaced by $\mathcal{N}_{\ker \partial_1}$ (Fig. 10(c) black, solid lines). The purpose of (73) is to recover the image representation form (pairwise interaction), which is accomplished using (54), allowing one to replace $\mathcal{N}_{\ker \partial_1}$ (Fig. 10(c) black, solid lines) with $\mathcal{N}_{\text{im } \partial_2}$ (Fig. 10(c) red, dashed lines). Finally, since the 2-torus lattice graph is self-dual, $\mathcal{N}_{\text{im } \partial_2}$ is identical to $\mathcal{N}_{\text{im } \partial_1}$, and so the resulting interaction system is an Ising model.

The key objects and key steps of the above comments are summarized in Fig. 13.

Proof. (Proof of Theorem 53.) Because $\mathcal{N}_{I(\tilde{\beta})}$ and $\mathcal{N}_{I(\tilde{\beta})}^h$ differ only in $L (= \sqrt{n})$ interaction functions, we have for any

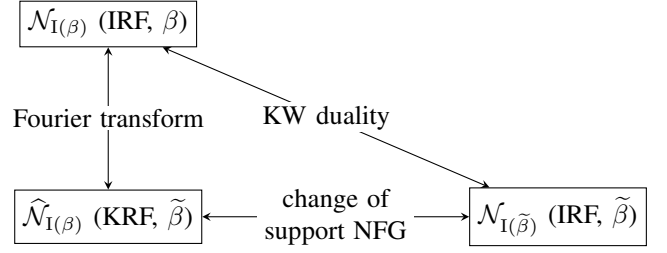


Fig. 13. Key objects and key steps of the Kramers–Wannier duality. The content of every box is “NFG (form, inverse temperature)”, where “NFG” refers to the relevant NFG, where “form” is either “IRF” (shorthand for “image-representation form”) or “KRF” (shorthand for “kernel-representation form”), and where “inverse temperature” refers to the inverse temperature appearing in the interaction functions.

configuration that the global function value for $\mathcal{N}_{I(\tilde{\beta})}^h$ is lower bounded by the global function value for $\mathcal{N}_{I(\tilde{\beta})}$ times $e^{-2\sqrt{n}\tilde{\beta}}$ and upper bounded by the global function value for $\mathcal{N}_{I(\tilde{\beta})}$ times $e^{+2\sqrt{n}\tilde{\beta}}$. Summing over all configurations, we obtain

$$Z_{\mathcal{N}_{I(\tilde{\beta})}} \cdot e^{-2\sqrt{n}\tilde{\beta}} \leq Z_{\mathcal{N}_{I(\tilde{\beta})}^h} \leq Z_{\mathcal{N}_{I(\tilde{\beta})}} \cdot e^{+2\sqrt{n}\tilde{\beta}},$$

i.e.,

$$\frac{1}{n} \log(Z_{\mathcal{N}_{I(\tilde{\beta})}}) - \frac{2\tilde{\beta}}{\sqrt{n}} \leq \frac{1}{n} \log(Z_{\mathcal{N}_{I(\tilde{\beta})}^h}) \leq \frac{1}{n} \log(Z_{\mathcal{N}_{I(\tilde{\beta})}}) + \frac{2\tilde{\beta}}{\sqrt{n}}.$$

Similarly,

$$\frac{1}{n} \log(Z_{\mathcal{N}_{I(\tilde{\beta})}}) - \frac{2\tilde{\beta}}{\sqrt{n}} \leq \frac{1}{n} \log(Z_{\mathcal{N}_{I(\tilde{\beta})}^v}) \leq \frac{1}{n} \log(Z_{\mathcal{N}_{I(\tilde{\beta})}}) + \frac{2\tilde{\beta}}{\sqrt{n}},$$

$$\frac{1}{n} \log(Z_{\mathcal{N}_{I(\tilde{\beta})}}) - \frac{4\tilde{\beta}}{\sqrt{n}} \leq \frac{1}{n} \log(Z_{\mathcal{N}_{I(\tilde{\beta})}^{hv}}) \leq \frac{1}{n} \log(Z_{\mathcal{N}_{I(\tilde{\beta})}}) + \frac{4\tilde{\beta}}{\sqrt{n}}.$$

For finite $\tilde{\beta}$, the desired result then follows by taking the limit $n \rightarrow \infty$ on both sides of (70), along with using the above inequalities to simplify the expression. \square

VII. EXTENSIONS

In this section, we discuss the Kramers–Wannier duality for some statistical models beyond the two-dimensional Ising model. There are two (independent) directions of extending the Ising model. Namely, on the one hand, one may look at higher-dimensional lattices, and, on the other hand, one may consider a different form of interaction functions between adjacent sites. We discuss the first direction in Section VII-A, which is about three-dimensional Ising models, and discuss the second direction in Section VII-B, which is about the Potts model [16].

A. Three-Dimensional Ising Models

In this section we consider different three-dimensional Ising type models and derive Kramers–Wannier type results. Note that we will first consider the cubic lattice before moving on to the 3-torus lattice graph.

A 3-complex, in addition to vertices, edges, and surfaces, also includes three-dimensional objects (polyhedra). We will denote the underlying graph by $\mathcal{G} \triangleq (\mathcal{V}, \mathcal{A}, \mathcal{S}, \mathcal{P})$, where \mathcal{P}

collects all polyhedra. The definition of the boundary of a vertex, edge, or a surface is similar to the 2-complex case, see Section IV-A. The boundary of a three-dimensional object $p \in \mathcal{P}$ is defined as the weighted sum of the surfaces surrounding p , where the weights are chosen from the set $\{-1, +1\}$ depending on the relative orientations of p and its surrounding surfaces.

Example 55. Consider the graph $\mathcal{G} \triangleq (\mathcal{V}, \mathcal{A}, \mathcal{S}, \mathcal{P})$ in Fig. 14(a) for which $\mathcal{P} = \{p_0\}$, i.e., it consists of a single polyhedron. (One can ignore the light blue dashed lines in the figure for the moment.) We choose the orientation (not shown in the figure) of the solid cube p_0 so that the front, left, and bottom faces have weight $+1$, and so that the back, right, and top faces have weight -1 in $\partial_3(p_0)$. One may verify that this results in the following 3-complex:

$$\begin{array}{ccccccc} & C_3 & \xrightarrow{\partial_3} & C_2 & \xrightarrow{\partial_2} & C_1 & \xrightarrow{\partial_1} & C_0 \\ \dim C_i & 1 & & 6 & & 12 & & 8 \\ \dim H_i & 0 & & 0 & & 0 & & 1 \end{array}$$

Some NFGs that are associated with this complex are shown in Figs. 14(b)–(g). (The choice of which NFGs are shown in the figure is based on which NFGs will be required for the subsequent discussions.)

The cube in Fig. 14(a) may be extended as part of a cubic lattice on a larger number of vertices in the obvious way, e.g., as done in Fig. 15(a). (The dashed lines in Fig. 14(a) show how the cube can be connected as part of a larger lattice.) In this case, the NFGs in Fig. 14 also extend in the obvious way, for instance, the NFGs $\mathcal{N}_{\text{im } \partial_3}$ and $\mathcal{N}_{\text{im } d_1}$ are as in Figs. 15(b) and (c), respectively. \triangle

The Ising model on the three-dimensional cubic lattice is defined in the same way as the two-dimensional Ising model, see the NFG $\mathcal{N}_{I(\beta)}$ in Fig. 16 (for now however without periodic boundary). Namely, the spins are located on the vertices of the cubic lattice, and we have the partition function Z as in (59), where now \mathcal{A} is the set of edges of the cubic lattice. The support NFG of $\mathcal{N}_{I(\beta)}$ is the NFG in Fig. 15(c). In subsequent discussions, we may simply refer to the corresponding NFGs in Fig. 14, where it is understood that the NFGs are extended to the appropriate number of vertices in the lattice.

In the three-dimensional Ising model, a spin (away from the borders of the lattice) has six neighbors, as can be seen in the NFG $\mathcal{N}_{I(\beta)}$ in Fig. 16. Now we can obtain a Kramers–Wannier type duality for the three-dimensional model as follows. (For reasons of simplicity, we omit the discussion of scaling factors.)

- We take the Fourier transform of the NFG $\mathcal{N}_{I(\beta)}$ in Fig. 16 (see Fig. 14(c) for the support NFG), which results in the NFG $\widehat{\mathcal{N}}_{I(\beta)}$ shown in Fig. 17 (see Fig. 14(e) for the support NFG). As in Section VI-C, we can relate the partition function of $\mathcal{N}_{I(\beta)}$ to the partition function of $\widehat{\mathcal{N}}_{I(\beta)}$.
- As in Section VI-C, the interaction functions of $\widehat{\mathcal{N}}_{I(\beta)}$ are in the desired form, but $\widehat{\mathcal{N}}_{I(\beta)}$ is in kernel-representation form because the support NFG of $\widehat{\mathcal{N}}_{I(\beta)}$ is equivalent to $\mathcal{N}_{\text{ker } \partial_1}$.

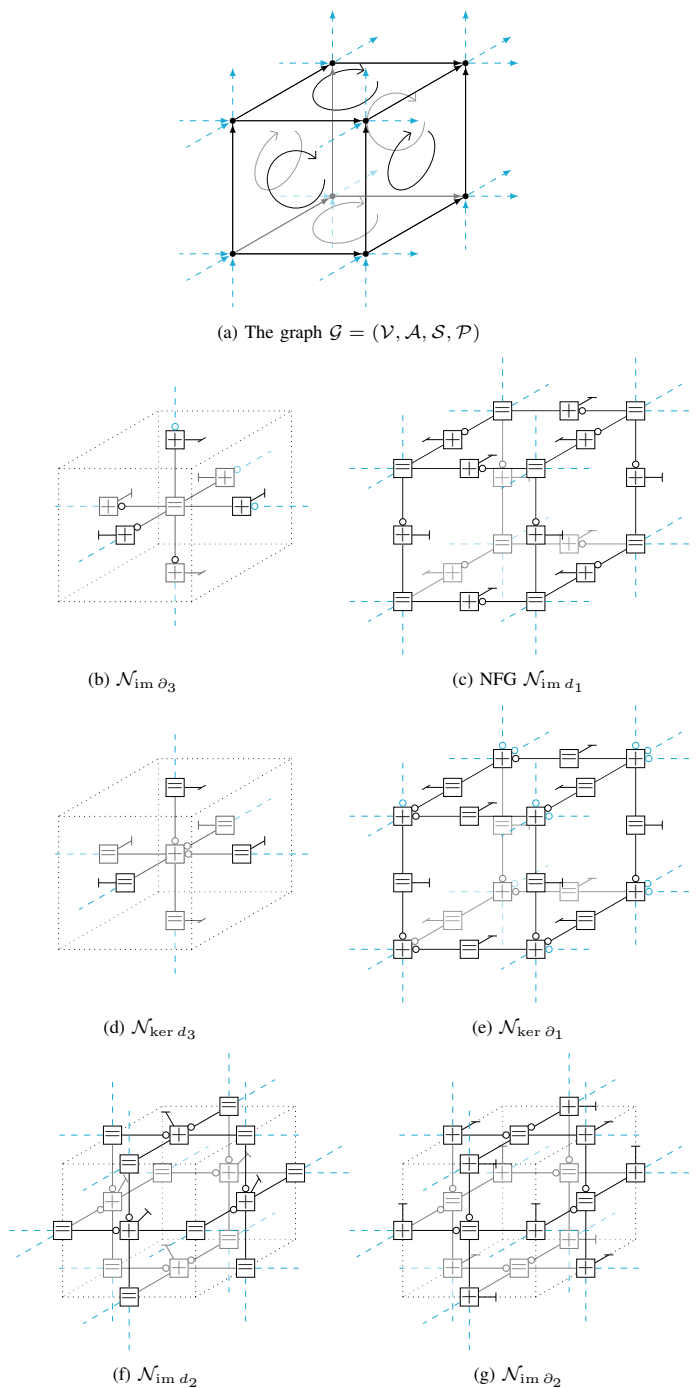


Fig. 14. A graph $\mathcal{G} = (\mathcal{V}, \mathcal{A}, \mathcal{S}, \mathcal{P})$ representing a cubic lattice and associated NFGs. (The dashed lines show how the figures extend for a larger lattice.)

lent to $\mathcal{N}_{\text{ker } \partial_1}$. In order to obtain an NFG in image-representation form, we replace the support NFG $\mathcal{N}_{\text{ker } \partial_1}$ (see Fig. 14(e) by $\mathcal{N}_{\text{im } d_2}$ (see Fig. 14(g)). Note that for the considered graph \mathcal{G} we have $\dim H_1 = 0$, i.e., $\mathcal{N}_{\text{ker } \partial_1}$ is equivalent to $\mathcal{N}_{\text{im } d_2}$.

In summary, we have been able to relate the partition functions of the following NFGs:

- 1) an NFG in image-representation form that represents some statistical model at inverse temperature β ;

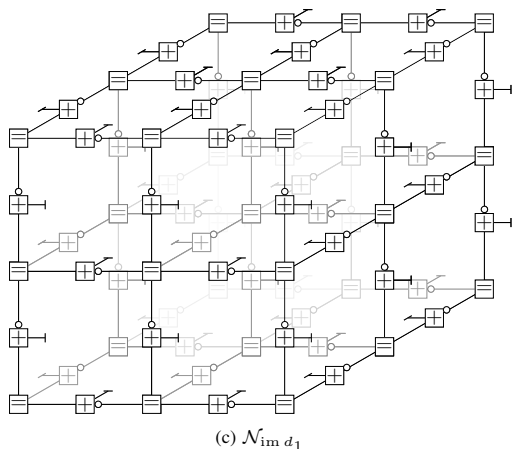
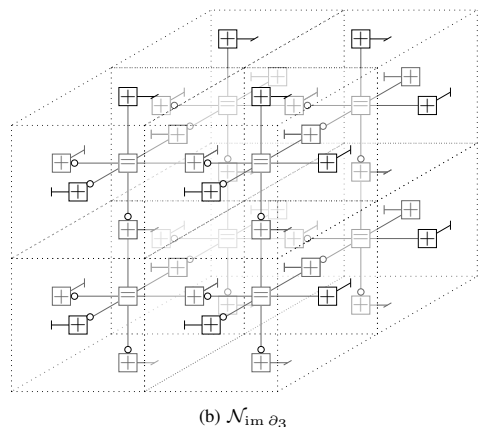
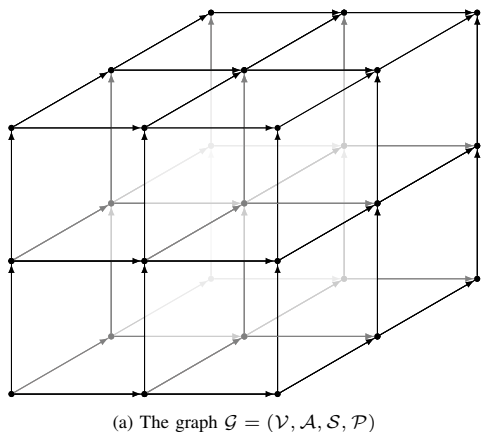


Fig. 15. A demonstration of some of the drawings in Fig. 14 for a larger cubic lattice.

- 2) an NFG in image-representation form that represents some other statistical model at the dual inverse temperature $\hat{\beta}$.

There are two key differences, however, to the analogous result in Section VI-C.

- In Section VI-C the connectivity pattern of the NFG corresponding to Item 2 was, due to the self-duality of the 2-torus lattice, the same as the connectivity pattern of the NFG corresponding to Item 1. This is not the case here anymore, i.e., the connectivity pattern of the NFG corresponding to Item 2 is different from the connectivity

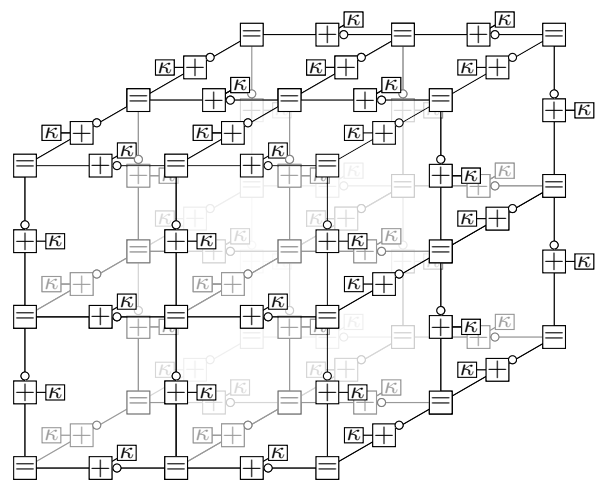


Fig. 16. The NFG $\mathcal{N}_{I(\beta)}$ representing the Ising model on the cubic lattice.

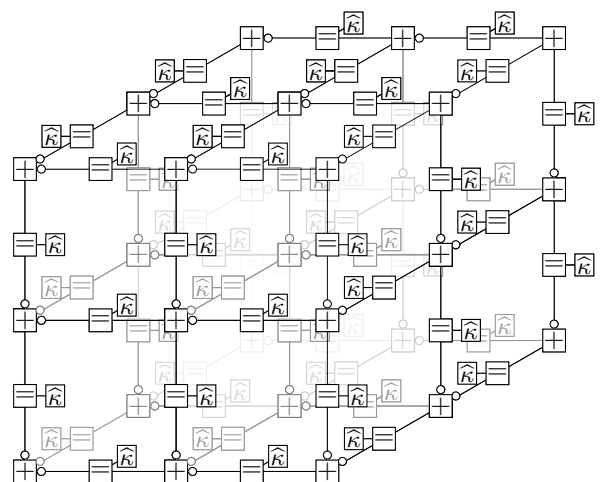


Fig. 17. The Fourier-transformed NFG $\hat{\mathcal{N}}_{I(\beta)}$.

pattern of the NFG corresponding to Item 1. In particular, in this section, whereas for the statistical model in Item 1 a spin (away from the borders of the lattice) interacts with 6 other spins, for the statistical model in Item 2 a spin (away from the borders of the lattice) interacts with 12 other spins.

- In Section VI-C the NFG corresponding to Item 2, since the lattice is two-dimensional, is a pairwise interaction NFG. (Like the NFG corresponding to Item 1.) This is not the case here anymore, i.e., the NFG corresponding to Item 2 is not a pairwise interaction NFG. (Unlike the corresponding NFG in Item 1) In particular, in this section, whereas for the statistical model in Item 1 an interaction function (away from the borders of the lattice) is connected to a parity indicator function that involves two spins, for the statistical model in Item 2, an interaction function is connected to a parity indicator function that involves four spins.

Finally, let us point out a different approach to obtain a Kramers–Wannier type duality result for the three-dimensional

Ising model. (In fact, this is the route taken by Savit in [10].) Namely, instead of placing spins at vertices and letting them interact via edges, we can place spins at the center of solid cubes and let them interact via their common face. A Kramers–Wannier type duality result is then obtained by considering the NFGs in Figs. 14(b)(d)(f) instead of Figs. 14(c)(e)(g). We omit the details.

Next, we proceed to the Ising model on the 3-torus lattice graph, where we start with the following example dedicated to the 3-complex obtained from the 3-torus.

Example 56. *The chain complex of the 3-torus lattice graph can be described using Fig. 18(a), obtained from Fig. 14(a) (ignoring the dashed edges) by identifying the left and right most faces, the top and bottom most faces, and the front and back most faces. Such an identification of the faces results in an identification of some corresponding edges and some corresponding vertices. Namely, in this case, all the vertices in Fig. 14(a) are identified as one vertex, all the horizontal edges as one edge, all the vertical edges as one edge, and all the perpendicular (to the page) edges as one edge, as shown in Fig. 18(a). Equivalently, this torus can be drawn as in Fig. 18(b). (By repeating vertices, edges, and faces.) Finally, the boundary operator is defined as in the previous example, and one may verify that one obtains the following 3-complex:*

$$\begin{array}{ccccccc} & C_3 & \xrightarrow{\partial_3} & C_2 & \xrightarrow{\partial_2} & C_1 & \xrightarrow{\partial_1} & C_0 \\ \dim C_i & 1 & & 3 & & 3 & & 1 \\ \dim H_i & 1 & & 3 & & 3 & & 1 \end{array}$$

Some NFGs that are associated with this complex are shown in Figs. 18(c)–(h).

Let $n \triangleq L^3$, where L is some positive integer. The cubic lattice with $L \times L \times L$ vertices on the 3-torus can be obtained via applying the identification above on the cubic lattice on $(L+1)^3$ vertices. As we have seen throughout this work, such a lattice will have the same dimensions of the homology spaces H_i as above. In other words, one may verify that the chain complex arising from the cubic lattice on the 3-torus may be summarized as

$$\begin{array}{ccccccc} & C_3 & \xrightarrow{\partial_3} & C_2 & \xrightarrow{\partial_2} & C_1 & \xrightarrow{\partial_1} & C_0 \\ \dim C_i & n & & 3n & & 3n & & n \\ \dim H_i & 1 & & 3 & & 3 & & 1 \end{array}$$

△

The corresponding NFGs to the ones in Fig. 18(c)–(h) for any n can be obtained in the obvious way, e.g., Figs. 19(a) and (b), respectively, show $\mathcal{N}_{\text{im } \partial_3}$ and $\mathcal{N}_{\text{im } \partial_1}$ for $n = 8$.

The Ising model on the 3-torus is shown in Fig. 20. The argument for a Kramers–Wannier type duality result is similar to the cubic lattice. However, while it is still true that $\text{im } \partial_2 \subseteq \ker \partial_1$, the reverse inclusion does not hold since $\dim H_1 = 3$, and we must take care of the cosets of $\text{im } \partial_2$ in $\ker \partial_1$. The approach is similar to the approach in Section VI-C, except that here we have $2^3 = 8$ cosets instead of $2^2 = 4$ cosets. We omit the details.

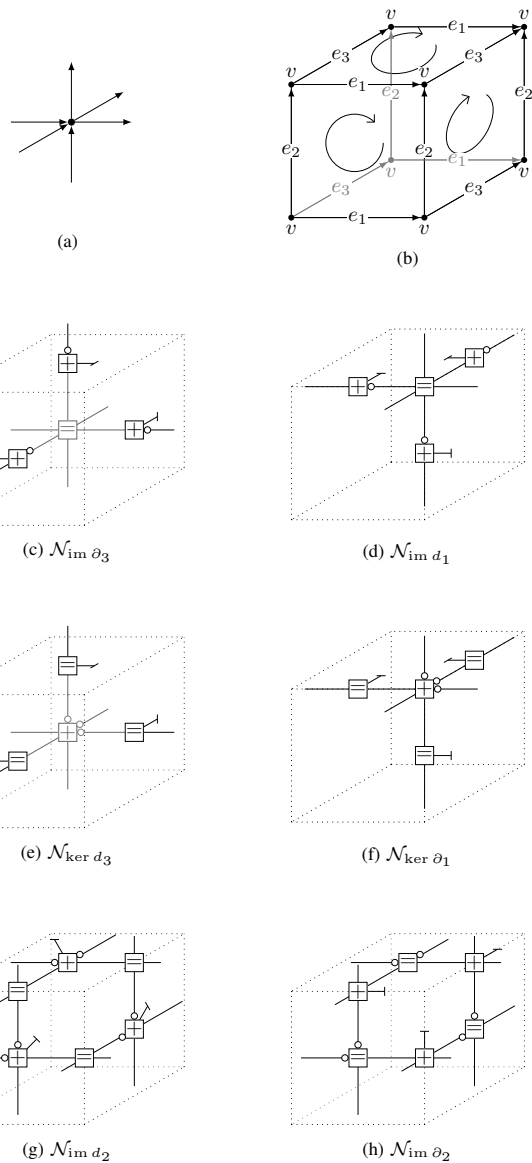


Fig. 18. A graph $\mathcal{G} = (\mathcal{V}, \mathcal{A}, \mathcal{S}, \mathcal{P})$ representing a 3-torus lattice graph and associated NFGs. In (a) and (c)–(h) the left and right most edges, the top and bottom most edges, and the front and back most edges are identified.

B. The Potts Model

In the Ising model on the 2-torus lattice, the spins are binary and the interaction between a pair of adjacent sites may take one of two values depending on whether the two spins are equal or not, i.e., the interaction depends on the Hamming distance between the pair of spins. An obvious extension is to allow spins to take values from a larger alphabet, which we will assume to be the ring \mathbb{Z}_q of integers modulo q , where $q \geq 2$ is an integer. While we still insist that the interaction may only depend on the difference between a pair of adjacent spins, there is certainly more freedom (compared to the Ising model) in choosing such a dependency, and several well-studied statistical models may be obtained by further specifying such a dependency. For instance, insisting on an interaction that only depends on the Hamming distance results in the standard Potts model, and specifying the interaction as

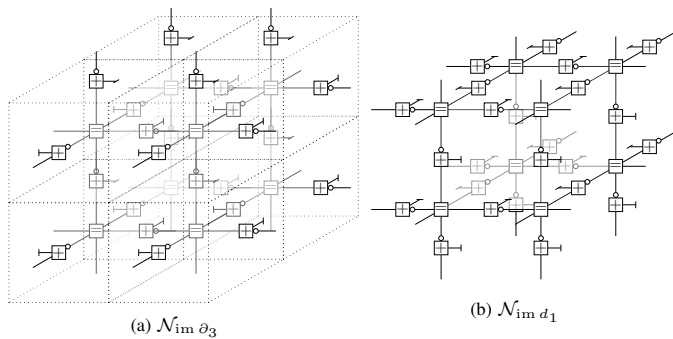


Fig. 19. A demonstration of some of the NFGs in Fig. 18 for the 3-torus with $n = 8$ vertices, where the edges follow the same identification as in Fig. 18

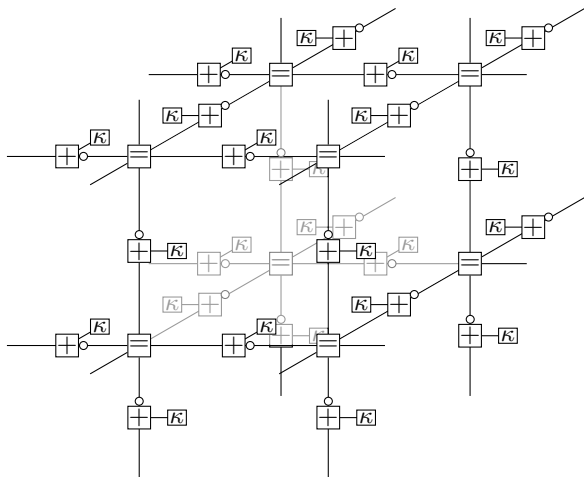


Fig. 20. The NFG \mathcal{G} representing the Ising model on the 3-torus with $n = 8$ sites, where the edges follow the same identification as in Fig. 18.

one that depends on the Lee distance gives the vector Potts model. For a detailed discussion of the Potts model [16], see, e.g., [17].

Note that most techniques from the previous sections can be suitably extended from a finite field \mathbb{F} to the ring \mathbb{Z}_q :

- The Fourier transform results still hold because they only rely on $(\mathbb{Z}_q, +)$ being a finite Abelian group.
- The results involving m -complexes need to be suitably generalized because vector spaces are replaced by modules.

It turns out that for the standard Potts model one can derive Kramers–Wannier type duality results. (We omit the rather straightforward details.) However, for the vector Potts model this does not seem to be the case. The issue here is that $\widehat{\kappa}_{\tilde{\beta}}$ cannot be expressed as some function $\kappa'_{\tilde{\beta}}$ such that $\tilde{\beta}^{-1} \cdot \log(\kappa'_{\tilde{\beta}})$ is independent of $\tilde{\beta}$, as would be required for the interaction function of a statistical model. (Exceptions are the special case $q = 3$, where the Lee distance reduces to the Hamming distance, and the special case $q = 4$, where one can show that the interaction decomposes into the Kronecker product of two interactions of binary spins.)

VIII. CONCLUSION

Over the last twenty years, factor graphs have proven to be a powerful concept. In contrast to many other diagrammatic representations that serve only a particular limited purpose, factor graphs have turned out to be very versatile: they can be applied in various contexts, they highlight how variables are related, they help us to efficiently do exact and approximate calculations, and they can be transformed. With the present paper, we have added another tool to this growing toolbox by showing how objects from algebraic topology can be expressed in terms of factor graphs and by discussing how algebraic topology can guide the transformation of factor graphs. We have then used these tools to re-prove the Kramers–Wannier duality. These tools have also proven to be beneficial in other contexts [14].

ACKNOWLEDGMENT

The authors gratefully acknowledge discussions with David Forney, Andi Loeliger, Yongyi Mao, and Mehdi Molkarai on topics related to this paper. In particular, the authors appreciate a comment in a paper by Molkarai and Loeliger [36] that started the investigations that led to the results discussed in the present paper and would also like to thank the reviewers and the associate editor for their valuable comments.

APPENDIX

A. Higher-Order Complexes

In Sections III–IV we have introduced 1-complexes and 2-complexes, respectively. The generalization to m -complexes for $m \geq 3$ is fairly straightforward and so this appendix is rather brief.

Let m be some positive integer. An m -dimensional chain complex, or simply m -complex, consists of the following objects:

- finite-dimensional spaces C_i over \mathbb{F} , $i \in \{-1, 0, 1, \dots, m+1\}$;
- boundary operators $\partial_i : C_i \rightarrow C_{i-1}$, $i \in \{0, 1, \dots, m+1\}$, where these operators satisfy

$$\text{im } \partial_{i+1} \subseteq \ker \partial_i, \quad i \in \{0, 1, \dots, m\},$$

i.e.,

$$\partial_i \circ \partial_{i+1} = 0, \quad i \in \{0, 1, \dots, m\}.$$

These objects are summarized in (74). For $i \in \{0, 1, \dots, m\}$, the i -th homology space is defined to be

$$H_i \triangleq \ker \partial_i / \text{im } \partial_{i+1}.$$

On the other hand, an m -dimensional cochain complex consists of the following objects:

- spaces \widehat{C}_i , $i \in \{-1, 0, 1, \dots, m+1\}$, where \widehat{C}_i is the dual space of C_i ;
- coboundary operators $d_i : \widehat{C}_{i-1} \rightarrow \widehat{C}_i$, $i \in \{0, 1, \dots, m+1\}$, where these operators satisfy

$$\text{im } d_i \subseteq \ker d_{i+1}, \quad i \in \{0, 1, \dots, m\}.$$

$$C_{m+1} \xrightarrow{\partial_{m+1}} C_m \xrightarrow{\partial_m} \dots \xrightarrow{\partial_3} C_2 \xrightarrow{\partial_2} C_1 \xrightarrow{\partial_1} C_0 \xrightarrow{\partial_0} C_{-1} \quad (74)$$

$$\widehat{C}_{m+1} \xleftarrow{d_{m+1}} \widehat{C}_m \xleftarrow{d_m} \dots \xleftarrow{d_3} \widehat{C}_2 \xleftarrow{d_2} \widehat{C}_1 \xleftarrow{d_1} \widehat{C}_0 \xleftarrow{d_0} \widehat{C}_{-1} \quad (75)$$

Fig. 21. Spaces and mappings associated with an m -complex.

i.e.,

$$d_{i+1} \circ d_i = 0, \quad i \in \{0, 1, \dots, m\}.$$

These objects are summarized in (75). For $i \in \{0, 1, \dots, m\}$, the i -th cohomology space is defined to be

$$\widehat{H}_i \triangleq \ker d_{i+1} / \operatorname{im} d_i.$$

The following list contains some further important notions:

- elements of C_i are called i -chains;
- elements of \widehat{C}_i are called i -cochains;
- elements of $\operatorname{im} \partial_{i+1}$ are called i -boundaries;
- elements of $\ker \partial_i$ are called i -cycles;
- elements of $\operatorname{im} d_i$ are called i -coboundaries;
- elements of $\ker d_{i+1}$ are called i -cocycles.

Finally, let us mention the useful fact that

$$\dim \widehat{H}_i = \dim H_i, \quad i \in \{0, 1, \dots, m\}. \quad (76)$$

This is a direct consequence of

$$\ker d_i = (\operatorname{im} \partial_i)^\perp, \quad (77)$$

$$\operatorname{im} d_i = (\ker \partial_i)^\perp, \quad (78)$$

where for any subspace $U \subseteq C_i$ we have defined its orthogonal space U^\perp to be

$$U^\perp \triangleq \{\varphi \in \widehat{C}_i \mid \varphi(x) = 0 \text{ for all } x \in U\}.$$

Equality (77) follows by noting that $\operatorname{im} \partial_i \subseteq C_{i-1}$, and so

$$\begin{aligned} (\operatorname{im} \partial_i)^\perp &= \{\varphi \in \widehat{C}_{i-1} \mid \varphi(x) = 0 \quad \forall x \in \operatorname{im} \partial_i\} \\ &= \{\varphi \in \widehat{C}_{i-1} \mid \varphi(\partial_i y) = 0 \quad \forall y \in C_i\} \\ &= \{\varphi \in \widehat{C}_{i-1} \mid (d_i \varphi)(y) = 0 \quad \forall y \in C_i\} \\ &= \ker d_i. \end{aligned}$$

(A similar argument leads to (78).) Now (76) follows easily from

$$\begin{aligned} \dim \widehat{H}_i &= \dim(\ker d_{i+1}) - \dim(\operatorname{im} d_i) \\ &= (\dim C_i - \dim(\operatorname{im} \partial_{i+1})) - (\dim C_i - \dim(\ker \partial_i)) \\ &= \dim H_i. \end{aligned}$$

REFERENCES

- [1] A. Al-Bashabsheh and P. O. Vontobel, "The Ising model: Kramers–Wannier duality and normal factor graphs," in *Proc. IEEE Int. Symp. on Inf. Theory*, Hong Kong, June 2015, pp. 2266–2270.
- [2] P. Bamberg and S. Sternberg, *A Course in Mathematics for Students of Physics*. Cambridge University Press, 1991, vol. 2.
- [3] A. Hatcher, *Algebraic Topology*. Cambridge, 2002.
- [4] J. R. Munkres, *Elements of Algebraic Topology*. Addison-Wesley, 1984.
- [5] F. R. Kschischang, B. J. Frey, and H.-A. Loeliger, "Factor graphs and the sum-product algorithm," *IEEE Trans. Inf. Theory*, vol. 47, no. 2, pp. 498–519, Feb. 2001.
- [6] H.-A. Loeliger, "An introduction to factor graphs," *IEEE Sig. Proc. Mag.*, vol. 21, no. 1, pp. 28–41, Jan. 2004.
- [7] G. D. Forney, Jr., "Codes on graphs: normal realizations," *IEEE Trans. Inf. Theory*, vol. 51, no. 2, pp. 520–548, Feb. 2001.
- [8] A. Al-Bashabsheh and Y. Mao, "Normal factor graphs and holographic transformations," *IEEE Trans. Inf. Theory*, vol. 57, no. 2, pp. 752–763, Feb. 2011.
- [9] H. Kramers and G. Wannier, "Statistics of the two-dimensional ferromagnet. Part I," *Physical Review*, vol. 60, no. 3, pp. 252–262, Aug. 1941.
- [10] R. Savit, "Duality in field theory and statistical systems," *Reviews of Modern Physics*, vol. 52, no. 2, pp. 453–487, April 1980.
- [11] K. Drühl and H. Wagner, "Algebraic formulation of duality transformations for abelian lattice models," *Annals of Physics*, vol. 141, no. 2, pp. 225–253, Feb. 1982.
- [12] E. Ising, "Beitrag zur Theorie des Ferromagnetismus," *Zeitschrift für Physik*, vol. 31, no. 1, pp. 253–258, 1925.
- [13] J. Maldacena, "The large N limit of superconformal field theories and supergravity," *Adv. Theor. Math. Phys.*, vol. 2, pp. 231–252, 1998.
- [14] J. X. Li and P. O. Vontobel, "Factor-graph representations of stabilizer quantum codes," in *Proc. 54th Allerton Conf. on Communication, Control, and Computing*, Allerton House, Monticello, IL, USA, Sep. 28–30 2016, pp. 1046–1053.
- [15] G. D. Forney, Jr., "Codes on graphs: models for elementary algebraic topology and statistical physics," July 2017, submitted to *IEEE Trans. Inf. Theory*, available online at arXiv:1707.06621.
- [16] R. B. Potts, "Some generalized order-disorder transformations," in *Mathematical Proceedings of the Cambridge Philosophical Society*, vol. 48, no. 1. Cambridge University Press, 1952, pp. 106–109.
- [17] F.-Y. Wu, "The Potts model," *Reviews of Modern Physics*, vol. 54, no. 1, pp. 235–268, 1982.
- [18] G. D. Forney, Jr. and P. O. Vontobel, "Partition functions of normal factor graphs," presented at the Inf. Theory Appl. Workshop, San Diego, CA, Feb. 2011.
- [19] P. O. Vontobel and H.-A. Loeliger, "On factor graphs and electrical networks," in *Mathematical Systems Theory in Biology, Communications, Computation, and Finance (IMA Volumes in Math. and Appl.)*, J. Rosenthal and D. Gilliam, Eds. New York: Springer Verlag, 2003, pp. 469–492.
- [20] Y. Mao and F. R. Kschischang, "On factor graphs and the Fourier transform," *IEEE Trans. Inf. Theory*, vol. 51, no. 5, pp. 1635–1649, 2005.
- [21] R. Lidl and H. Niederreiter, *Finite Fields*, ser. Encyclopedia of Mathematics and its Applications. Cambridge University Press, 1997, vol. 20.
- [22] G. D. Forney, Jr., "Private communications," 2015.
- [23] R. Tanner, "A recursive approach to low complexity codes," *IEEE Trans. Inf. Theory*, vol. 27, no. 5, pp. 533–547, Sept. 1981.
- [24] N. Wiberg, H.-A. Loeliger, and R. Kötter, "Codes and iterative decoding on general graphs," *Euro. Trans. Telecom.*, vol. 6, no. 5, pp. 513–525, Sept./Oct. 1995.
- [25] A. Y. Kitaev, "Fault-tolerant quantum computation by anyons," *Annals of Physics*, vol. 303, no. 1, pp. 2–30, 2003.
- [26] R. J. Baxter, *Exactly Solved Models in Statistical Mechanics*. Courier Dover Publications, 2007.
- [27] A. Kato and K. Zeger, "On the capacity of two-dimensional run-length constrained channels," *IEEE Trans. Inf. Theory*, vol. 45, no. 5, pp. 1527–1540, July 1999.
- [28] H. Whitney, "The coloring of graphs," *Annals of Mathematics*, pp. 688–718, Oct. 1932.
- [29] A. Barvinok, *Combinatorics and Complexity of Partition Functions*. Cham, Switzerland: Springer, 2016.
- [30] G. Potamianos and J. Goutsias, "Stochastic approximation algorithms for partition function estimation of Gibbs random fields," *IEEE Trans. Inf. Theory*, vol. 43, no. 6, pp. 1948–1965, Nov. 1997.
- [31] L. P. Kadanoff, "Scaling laws for Ising models near T_c ," *Physics*, vol. 2, no. 6, pp. 263–272, Feb. 1966.
- [32] K. G. Wilson, "Renormalization group and critical phenomena. I. Renormalization group and the Kadanoff scaling picture," *Physical Review B*, vol. 4, no. 9, pp. 3174–3184, Nov. 1971.
- [33] H. Bethe, "Statistical theory of superlattices," *Proc. Roy. Soc. London A*, vol. 150, no. 871, pp. 552–575, Feb. 1935.
- [34] M. J. Wainwright, T. S. Jaakkola, and A. S. Willsky, "A new class of upper bounds on the log partition function," *IEEE Trans. Inf. Theory*, vol. 51, no. 7, pp. 2313–2335, July 2005.

- [35] M. Jerrum and A. Sinclair, "Polynomial-time approximation algorithms for the Ising model," *SIAM Journal on Computing*, vol. 22, no. 5, pp. 1087–1116, 1993.
- [36] M. Molkaraie and H.-A. Loeliger, "Partition function of the Ising model via factor graph duality," in *Proc. IEEE Int. Symp. Inf. Theory*, Istanbul, Turkey, July 2013, pp. 2304–2308.
- [37] A. Al-Bashabsheh and Y. Mao, "On stochastic estimation of the partition function," in *Proc. IEEE Int. Symp. on Inf. Theory*, Honolulu, HI, June 2014, pp. 1504–1508.

Ali Al-Bashabsheh received a B.Sc. (2001) and an M.Sc. (2005) in electrical engineering from Jordan University of Science and Technology, an M.Sc. (2012) in mathematics from Carleton University, and a Ph.D. (2014) in electrical engineering from the University of Ottawa. His research interests include graphical models, information theory, and machine learning.

Pascal O. Vontobel (S'96–M'97–SM'12) received the Diploma degree in electrical engineering in 1997, the Post-Diploma degree in information techniques in 2002, and the Ph.D. degree in electrical engineering in 2003, all from ETH Zurich, Switzerland.

From 1997 to 2002 he was a research and teaching assistant at the Signal and Information Processing Laboratory at ETH Zurich, from 2006 to 2013 he was a research scientist with the Information Theory Research Group at Hewlett-Packard Laboratories in Palo Alto, CA, USA, and since 2014 he has been an Associate Professor at the Department of Information Engineering at the Chinese University of Hong Kong. Besides this, he was a postdoctoral research associate at the University of Illinois at Urbana-Champaign (2002–2004), a visiting assistant professor at the University of Wisconsin-Madison (2004–2005), a postdoctoral research associate at the Massachusetts Institute of Technology (2006), and a visiting scholar at Stanford University (2014). His research interests lie in coding and information theory, quantum information processing, data science, communications, and signal processing.

Dr. Vontobel has been an Associate Editor for the IEEE TRANSACTIONS ON INFORMATION THEORY (2009–2012) and the IEEE TRANSACTIONS ON COMMUNICATIONS (2014–2017), an Awards Committee Member of the IEEE Information Theory Society (2013–2014), a Distinguished Lecturer of the IEEE Information Theory Society (2014–2015), and a TPC co-chair of the 2016 IEEE International Symposium on Information Theory. Currently, he is a TPC co-chair of the upcoming 2018 IEICE International Symposium on Information Theory and its Applications in Singapore and of the upcoming 2018 IEEE Information Theory Workshop in Guangzhou, China. He has been on the technical program committees of many international conferences and has co-organized several topical workshops. Moreover, he has been three times a plenary speaker at international information and coding theory conferences and has been awarded the ETH medal for his Ph.D. dissertation.